ABSTRACT

Title of Thesis: ADVANCES TO A COMPUTER MODEL USED IN THE SIMULATION AND OPTIMIZATION OF HEAT EXCHANGERS

Robert Andrew Schwentker, Master of Science, 2005

Thesis Directed By: Professor Reinhard Radermacher
Department of Mechanical Engineering

Heat exchangers play an important role in a variety of energy conversion applications. They have a significant impact on the energy efficiency, cost, size, and weight of energy conversion systems. CoilDesigner is a software program introduced by Jiang (2003) for simulating and optimizing heat exchangers. This thesis details advances that have been made to CoilDesigner to increase its accuracy, flexibility, and usability.

CoilDesigner now has the capability of modeling wire-and-tube condensers under both natural and forced convection conditions on the air side. A model for flat tube heat exchangers of the type used in automotive applications has also been developed. Void fraction models have been included to aid in the calculation of charge. In addition, the ability to model oil retention and oil's effects on fluid flow and heat transfer has been included. CoilDesigner predictions have been validated with experimental data and heat exchanger optimization studies have been performed.

ADVANCES TO A COMPUTER MODEL USED IN THE SIMULATION AND OPTIMIZATION OF HEAT EXCHANGERS

by

Robert Andrew Schwentker

Thesis submitted to the Faculty of the Graduate School of the
University of Maryland, College Park in partial fulfillment
of the requirements for the degree of
Master of Science
2005

Advisory Committee:

Professor Reinhard Radermacher, Chair
Associate Professor Linda Schmidt
Assistant Professor Bao Yang

Dedication

Dedicated
to
my wife

Acknowledgements

I would first like to express my deep gratitude to my advisor, Dr. Reinhard Radermacher, for enabling me to study and conduct research at the University of Maryland, College Park. His support and faith in my abilities over the past couple of years are greatly appreciated. I would also like to thank Dr. Linda Schmidt and Dr. Bao Yang for serving on my thesis committee and for providing valuable comments regarding my thesis.

I am very grateful to my colleagues I have worked closely with, including Vikrant Aute, Lorenzo Cremaschi, John Fogle, Amr Gado, Ersin Gerçek, Kai Hübner, Ahmet Ors, Jon Winkler, and Eric Xuan. They have all been very helpful and have made the time I spent at the University of Maryland much more enjoyable.

I would also like to thank the companies that support the Center for Environmental Energy Engineering at the University of Maryland for making the research presented in this thesis possible.

Finally, I would like to thank my parents, my brother, and my wife. Without their love and support, this work would not have been possible. I am deeply grateful to all of them.

Table of Contents

List of Tables

List of Figures

Nomenclature

A	Area (m^2)
$A_{frontal}$	Frontal face area of heat exchanger (m^2)
A_{min}	Minimum free flow area (m^2)
C	Constant
c_p	Specific heat (J kg^{-1} K^{-1})
D	Diameter (m)
f	Friction factor
F_p	Fin pitch (m)
H	Heat exchanger height (m)
G	Mass flux (kg m^{-2} s^{-1})
g	Acceleration due to gravity, 9.81 (m s^{-2})
h	Heat transfer coefficient (W m^{-2} K^{-1})
j	Colburn factor
k	Thermal conductivity (W m^{-1} K^{-1})
L_θ	Louver angle (degrees)
L_h	Louver height (m)
L_l	Louver length (m)
L_p	Louver pitch (m)
$\dot{m}$	Mass flow rate (kg s^{-1})
N	Fan rotational speed (rev min^{-1})
NTU	Number of transfer units
Nu	Nusselt number
P	Pressure (Pa)
p	Perimeter (m)
p	Pitch (m)
Pr	Prandtl number, $\mu \cdot c_p / k$
Q	Heat duty (W), Volumetric air flow rate (m^3 s^{-1})
R	Heat transfer resistance
Ra	Rayleigh number
Re	Reynolds number
S	Slip ratio
S_l	Tube horizontal spacing (m)
S_t	Tube vertical spacing (m)
S_w	Wire spacing (m)
St	Stanton number
T	Temperature (K)
T_h	Tube height (m)
T_w	Tube width (m)
UA	Overall heat transfer conductance
v	Velocity (m s^{-1})
W	Molecular mass, Fan power consumption (W)
We	Weber number

Greek

β	Thermal expansion coefficient (K^{-1})
δ	Liquid film thickness (m)
ε	Heat exchange effectiveness
η	Fin efficiency
η_s	Surface effectiveness
μ	Viscosity (kg m^{-1} s^{-1})
ξ	Yokozeki factor
ρ	Density (kg m^{-3})
σ	Surface tension (N m^{-1})
σ	Stefan-Boltzmann constant, 5.67×10^{-8} (W K^{-4} m^{-2})
Ψ	mole fraction

Subscript

a	air
c	Convective
in	Inlet, Inner
liq	Liquid
out	Outlet, Outer
r	Radiative
ref	Refrigerant
t	Tube
vap	Vapor, Gas
w	Wire

Chapter 1 Introduction

1.1 Overview

Over the past several years, with energy costs rising and awareness of the environmental impact of the use of fossil fuels increasing, there has been a greater focus around the world on energy usage and consumption. Increasing the efficiency of energy-intensive products and processes is one of the most important methods available for confronting and reducing the problems associated with energy consumption. By increasing energy efficiency, traditional energy supplies will last longer and the harmful effects related to energy consumption, such as global warming, can be reduced.

Vapor compression systems used in heating, ventilating, air-conditioning, and refrigerating (HVAC&R) applications are energy-intensive and represent a significant portion of the total energy consumption of buildings and automobiles. Much progress has been made over the past couple of decades to improve the energy efficiency of such systems. However, research continues and more progress can be achieved.

As computer processing power has increased, the ability to use simulation software for engineering purposes has increased dramatically. This is true of vapor compression systems, as well. The use of software simulation tools is an increasingly popular method for improving the efficiency of vapor compression systems. This can be performed through the use of system-level simulation tools as well as component-level simulation tools. Heat exchanger simulation is particularly important because heat exchangers comprise two of the four major components of vapor compression

systems. Therefore, it is important to develop a simulations tool that can be used to design, simulate, and optimize heat exchangers.

The cost associated with designing and manufacturing heat exchangers is also of major concern. The price of raw materials used in heat exchangers, such as aluminum and copper, have been rising over the past few years as demand has increased in countries such as China and India. Moreover, manufacturers now have to compete with companies from around the globe, making costs a more important factor than ever. The use of simulation software can reduce the cost and time required to design heat exchangers for new systems. Instead of building multiple prototype heat exchangers and testing each one, multiple heat exchanger designs can be modeled and then a couple of the best designs can be built and tested. This aids in the design of heat exchangers that will perform as needed on the first try. Heat exchanger simulation tools can also be used to perform optimization studies in order to decrease the material and cost necessary to manufacture heat exchangers.

Heat exchangers are also used in a variety of applications beyond HVAC&R systems. They are also used for thermal management in automobiles as well as in applications in food processing, petrochemical, textile, and other process industries. Therefore, a heat exchanger simulation tool can have a variety of applications.

CoilDesigner is a software simulation tool used for the simulation and optimization of heat exchangers that was first introduced by Jiang (2003). Its most distinguishing features include its generality, the level of detail, and its user-friendly graphic interface. At that time, CoilDesigner could be used to model two types of heat exchanger often used in HVAC&R systems—round tube plate fin (RTPF) heat

exchangers and microchannel heat exchangers. Jiang also validated the RTPF model with experimentally measured data. Over the past couple of years, further research has been performed to increase the number of applications and the accuracy of CoilDesigner. In this thesis, advances that have been made to CoilDesigner are detailed.

1.2 Objectives of Research

The primary objective of this thesis is to detail advances that have been made to CoilDesigner. The specific objectives of this research include the following:

- Develop two new heat exchanger models in addition to the two pre-existing heat exchanger models:
    - Develop a model that can simulate wire-and-tube condensers of the type used in refrigerators. Include the ability to model natural convection heat transfer as well as forced convection heat transfer on the air side.
    - Develop a model that can simulate flat tube heat exchangers of the type used in automotive applications for radiators and charge air coolers.
- Implement new fluid modeling capabilities:
    - Research various void fraction models and implement them in CoilDesigner for the accurate calculation of refrigerant charge.
    - Implement the ability to model refrigerant-oil mixtures in heat exchangers by accomplishing the following:

    - Include correlations and procedures to calculate the heat transfer as well as the thermodynamic and physical properties of refrigerant-oil mixtures.
    - Include correlations developed specifically for refrigerant-oil mixtures to calculate heat transfer coefficients and pressure drop.
    - Calculate oil retention in heat exchangers with the use of void fraction models.
- Perform validation and optimization studies with CoilDesigner:
    - Validate the microchannel heat exchanger model with experimental heat exchanger performance data.
    - Validate the wire-and-tube condenser model with experimental heat exchanger performance data.
    - Use experimental data to validate the refrigerant-oil model and its ability to calculate oil retention.
    - Perform optimization studies of a wire-and-tube condenser to increase performance and reduce cost.

Chapter 2 Heat Exchanger Modeling

The general modeling techniques employed in CoilDesigner have been detailed by Jiang (2003). This chapter discusses the main concepts and equations in order to provide the reader with enough background knowledge to be able to contextualize the advances made to CoilDesigner.

To model a heat exchanger, CoilDesigner uses a segment-by-segment approach in which each tube is divided into multiple segments and the hydraulic and heat transfer/energy equations are solved for each segment individually. Dividing each tube into multiple segments allows two-dimensional non-uniformity of air distribution to be modeled because different values for air velocity and temperature can be input for each segment. Dividing tubes into segments also allows heterogeneous refrigerant flow through a tube to be modeled, increasing the accuracy of the heat exchanger model.

Each tube is divided into multiple segments, and then each segment is treated like a small cross-flow heat exchanger. The air-to-refrigerant heat transfer and the refrigerant pressure drop are calculated for each individual segment. On the refrigerant side, each segment is provided with an inlet enthalpy, an inlet pressure, and a mass flow rate. On the air side, the inlet air temperature is provided for each segment. The inlet air flow rate is also provided for each segment when modeling heat transfer of heat exchangers undergoing forced convection on the air side.

2.1 Modeling of the Refrigerant Side

The heat transfer between the refrigerant and the walls of the tubes through which the refrigerant flows is governed by the temperature gradient and a heat transfer coefficient:

$$q = h \cdot A \cdot \left(T_{ref} - T_{wall}\right) \tag{2.1}$$

In steady state, the heat transfer from the refrigerant to the walls must equal the overall heat transfer from the refrigerant to the air. Therefore, in order to model the heat transfer between the refrigerant and the air in heat exchangers, a heat transfer coefficient must be calculated for the refrigerant as it flows through the tubes. Multiple theoretical and empirical correlations have been developed over the past several decades to model heat transfer coefficients for different geometric parameters, flow regimes, refrigerants, operating conditions, and processes (i.e. if the refrigerant is undergoing evaporation or condensation). These correlations are typically of the form

$$h = \rho v c_p St \tag{2.2}$$

in which St is the Stanton Number

$$St = \frac{j}{Pr^{2/3}} \tag{2.3}$$

Correlations included in CoilDesigner are discussed by Jiang (2003). Some additional correlations that have been included in CoilDesigner over the last couple of years are discussed in the Appendix.

The pressure drop of the refrigerant as it flows through the heat exchanger must also be modeled because of the significant impact both on the power

consumption of HVAC&R systems and on the thermodynamic and transport properties of the refrigerant. As discussed by Jiang (2003), the accelerational and gravitational components of the pressure drop are dominated by the frictional pressure drop and can therefore be neglected. Thus, the pressure drop can be expressed by the equation

$$P_{in} - P_{out} = \Delta P = f \frac{2L}{\pi \rho D^3} \dot{m}^2 \tag{2.4}$$

where f is a friction factor. Just as for heat transfer coefficients, multiple correlations have been developed to model the friction factor for different geometric parameters, flow regimes, refrigerants, and operating conditions. Correlations included in CoilDesigner are discussed by Jiang (2003) and correlations that have been added are detailed in the Appendix.

2.2 Modeling of Heat Transfer Between Refrigerant and Air

For each segment of a tube, the energy balance equation for the refrigerant is described by the following equation:

$$q = \dot{m}_{ref} \left(h_{ref,out} - h_{ref,in} \right) \tag{2.5}$$

where h_{ref} is the enthalpy of the refrigerant. In the case of single-phase refrigerant, the equation can be approximated as

$$q = \dot{m}_{ref} c_{p,ref} \left(T_{ref,out} - T_{ref,in} \right) \tag{2.6}$$

The energy balance equation for the air side is described by the following equation:

$$q = \dot{m}_{air} \left(h_{air,in} - h_{air,out} \right) = \dot{m}_{air} c_{p,air} \left(T_{air,in} - T_{air,out} \right) \tag{2.7}$$

In order to use these energy balance equations to calculate the heat transfer between the air and the refrigerant, a method is needed to calculate the outlet temperatures. The ε-NTU method for cross-flow configuration with one fluid mixed and the other fluid unmixed is used for this purpose (Kays and London, 1984). The refrigerant is modeled as a mixed fluid and the air is modeled as an unmixed fluid. The heat capacities of each fluid are

$$C_{mixed} = \dot{m}_{ref} c_{p,ref} \tag{2.8}$$

$$C_{unmixed} = \dot{m}_{air} c_{p,air} \tag{2.9}$$

and the number of heat transfer units, *NTU*, is defined as:

$$NTU = \frac{UA}{C_{\min}} \tag{2.10}$$

UA is an overall heat conductance which is calculated using the idea of a thermal circuit (Myers, 1998):

$$\frac{1}{UA} = \frac{1}{h_{ref} \cdot A_{t,in}} + \frac{R_{thermal}}{A_{t,out}} + \frac{R_{contact}}{A_{t,out}} + \frac{R_{fouling}}{A_{t,out}} + \frac{1}{h_{air} \cdot \eta_s \cdot A_{total,out}} \tag{2.11}$$

where $R_{thermal}$, $R_{contact}$, and $R_{fouling}$ are thermal, contact, and fouling resistances that can be input by the user, and η_s is the surface effectiveness of the heat exchanger. This surface effectiveness is a function of the fin efficiency, η_f, as well as of the outer surface areas of the tubes and fins, and is calculated according to the following equation:

$$\eta_s = \frac{A_{t,out} + \eta_f A_f}{A_{total}} \tag{2.12}$$

Correlations are available to predict refrigerant-side and air-side heat transfer coefficients as well as fin efficiencies needed for Eq. 2.11. The correlations are

typically developed based on empirical measurements and are functions of geometrical parameters and flow characteristics. Details of correlations that have been added to CoilDesigner are provided in the Appendix.

The heat exchange effectiveness, ε, is the ratio of the change in temperature, ΔT, to the maximum possible temperature change, based on the inlet temperatures of the two fluids. ε is calculated for each segment depending on the heat capacities, C, for each fluid. For the case in which $C_{max} = C_{unmixed}$ (in other words, when the air has the higher heat capacity),

$$\varepsilon = 1 - \exp\left\{ -\frac{C_{max}}{C_{min}} \left[1 - \exp\left(-NTU \frac{C_{min}}{C_{max}} \right) \right] \right\} \tag{2.13}$$

and

$$\varepsilon = \frac{T_{ref,in} - T_{ref,out}}{T_{ref,in} - T_{air,in}} \tag{2.14}$$

On the other hand, for $C_{max} = C_{mixed}$,

$$\varepsilon = \frac{C_{max}}{C_{min}} \left\{ 1 - \exp\left[-\frac{C_{min}}{C_{max}} \left(1 - \exp\left(-NTU \right) \right) \right] \right\} \tag{2.15}$$

and

$$\varepsilon = \frac{T_{air,out} - T_{air,in}}{T_{ref,in} - T_{air,in}} \tag{2.16}$$

When the refrigerant in a segment is in the two-phase regime,

$$\frac{C_{min}}{C_{max}} = 0 \tag{2.17}$$

$$\varepsilon = 1 - \exp\left(-NTU \right) \tag{2.18}$$

Once ε is calculated for the segment, the outlet temperature of either the air or the refrigerant can be calculated by rearranging Eq. 2.14 or Eq. 2.16. In the case of two-phase refrigerant flowing through the segment, Eq. 2.16 must be used to calculate the outlet air temperature because the refrigerant temperature remains constant during the evaporation or condensation process. After calculating the outlet air temperature, the heat load of the segment can then be calculated using Eq. 2.7.

2.3 Subdivided Segment Model

As discussed before, in CoilDesigner, tubes are divided into multiple segments for solving the energy balance and the hydraulic equations. Typically, it can be assumed that the refrigerant flowing through a segment does not undergo a change in flow regime. A segment is usually occupied entirely by superheated vapor, two-phase fluid, or subcooled liquid. However, there may be segments in which the refrigerant undergoes a flow regime change, as shown in Figure 2-1. In order to account for the significant changes in the refrigerant properties and the heat transfer coefficients, a subdivided segment model is included in CoilDesigner in which the segment is divided further into sub-segments, each of which is occupied entirely by either single phase or two-phase refrigerant.

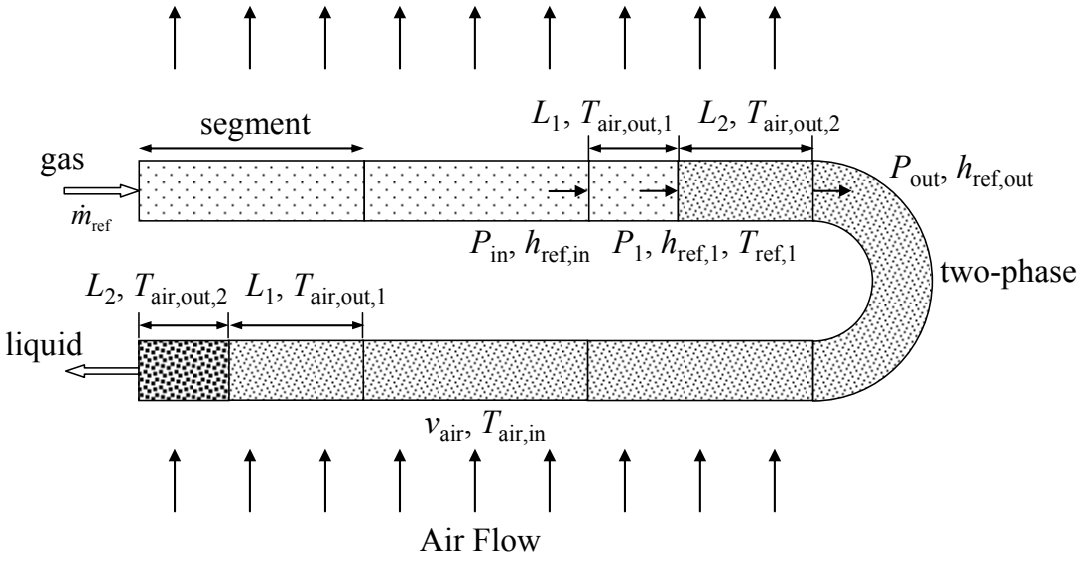

Figure 2-1. Drawing of refrigerant undergoing phase changes within segments

The ε-NTU equations presented above are modified as follows. If x is the fraction of the length of the segment at which a flow regime change takes place, then the heat capacities and *NTU* for the sub-segment are calculated according to the following equations:

$$C_{mixed} = \dot{m}_{ref} c_{p,ref} \tag{2.19}$$

$$C_{unmixed} = x\dot{m}_{air} c_{p,air} \tag{2.20}$$

$$NTU = x\frac{UA}{C_{\min}} \tag{2.21}$$

As before, the heat exchange effectiveness, ε, is calculated using Eq. 2.13, 2.15, or 2.18, depending on which is appropriate according to the relationship between C_{mixed} and C_{unmixed}. The following equations can then be used to calculate the outlet temperatures of the first sub-segment:

$$\varepsilon = \frac{T_{ref,in} - T_{ref,1}}{T_{ref,in} - T_{air,in}} \tag{2.22}$$

$$\varepsilon = \frac{T_{air,out,1} - T_{air,in}}{T_{ref,in} - T_{air,in}} \tag{2.23}$$

The heat load of the first sub-segment is governed by the equation

$$q = x\dot{m}_{air} c_{p,air} \cdot \left(T_{air,out,1}(x) - T_{air,in}\right) = \dot{m}_{ref} \cdot \left(h_{ref,in} - h_{ref,1}\right) \tag{2.24}$$

where $h_{ref,1}$, the enthalpy at the interface between sub-segments, is the saturated enthalpy of the refrigerant given the pressure, P_1, at the interface:

$$h_{ref,1}(x) = h_{sat}\left(P_{ref,1}(x)\right) \tag{2.25}$$

$$P_{ref,1}(x) = P_{ref,in} - \Delta P\left(x, P_{ref,in}, h_{ref,in}\right) \tag{2.26}$$

This set of equations, Eqs. 2.19 through 2.26, reduces to one equation with x being the unknown. The implicit equation is solved using a numerical iteration scheme. Once x is calculated, the refrigerant pressure and enthalpy and the air temperature at the outlet of the sub-segment are known. The ε-NTU method is then used to calculate the heat load of the next sub-segment. Then the outlet conditions of the entire segment can be calculated.

Chapter 3 Wire-and-Tube Condenser Model

Wire-and-tube condensers have been used in domestic refrigerators for decades. This type of condenser consists of a single steel tube bent into a serpentine tube bundle with pairs of steel wires welded onto opposite sides of the tube to serve as extended surfaces. Wire-and-tube condensers employ either natural convection or forced convection heat transfer on the air side. Natural convection wire-and-tube condensers typically consist of a single bank attached to the back of a refrigerator. They are coated in black paint to increase the emissivity to increase the radiation heat transfer. As the air around the tubes is heated, its density decreases and it begins to rise, causing upward-moving turbulent air flow resulting in convective heat transfer. Forced convection wire-and-tube condensers typically are in the form of a tube bundle consisting of several rows and several banks, and they have a fan forcing air circulation through the heat exchanger.

Despite the prevalence of wire-and-tube condensers and their central role in the efficiency and cost of refrigerators, very little literature has been published about modeling them. The refrigerant-side heat transfer coefficients and pressure drop can be modeled using the same equations and correlations as for traditional round tube plate fin heat exchangers. However, in order to be able to model this type of heat exchanger and to be able to perform optimization studies, accurate models for heat transfer to the air, and therefore the air-side heat transfer coefficient and the fin efficiency are needed.

A few articles have been published in recent years on modeling natural convection wire-and-tube condensers. Tanda and Tagliafico (1997) developed a

correlation to predict the natural convection heat transfer coefficient for wire-and-tube condensers with vertical wires attached to a single column of tubes. Tanda and Tagliafico obtained experimental data by measuring the heat transfer from water flowing through wire-and-tube heat exchangers. In order to minimize the effects of radiative heat transfer during their experiments, they coated the heat exchangers with low-emissivity paint. They then calculated theoretically the contribution from radiative heat transfer and subtracted it from the total heat transfer before calculating the natural convection heat transfer coefficient. They developed a semi-empirical heat transfer coefficient correlation as a function of geometric and operating parameters.

Tagliafico and Tanda (1997) also presented a wire-and-tube condenser model that accounted for both natural convection and radiation heat transfer. They used the semi-empirical correlation presented in their previous paper (Tanda and Tagliafico, 1997) to model the natural convection heat transfer coefficient. For radiation heat transfer, they developed a theoretical model to calculate the average radiation heat transfer coefficient. The authors then validated their model with a second set of experimental data from eight wire-and-tube condensers with widely varying geometric parameters.

Quadir *et al*. (2002) also developed a wire-and-tube condenser model for natural convection. They used a finite element method and modeled varying ambient temperatures and refrigerant flow rates in order to examine the effects on heat exchanger performance. The authors assumed a constant overall heat transfer coefficient of 10 W/m^2 K.

Bansal and Chin (2003) developed a computer model for natural convection using a finite element and variable conductance approach written in FORTRAN 90. The authors used the natural convection heat transfer coefficient correlation developed by Tagliafico and Tanda (1997). Bansal and Chin also used the same theoretical approach presented by Tagliafico and Tanda to calculate the radiative heat transfer coefficient. The authors used these air-side heat transfer coefficients as well as the thermal conductivity of the tube and the refrigerant-side heat transfer coefficient to calculate an overall heat transfer conductance value, *UA*. They used the *UA* value in calculating the total heat transfer of each finite element of the heat exchanger. The paper also contains an iterative computational scheme that the authors used to calculate the total heat transfer, pressure drop, and outlet conditions of wire-and-tube condensers. The authors validated their computer model using their own experimental data. They then used their computer model to optimize a wire-and-tube condenser.

To the current author's knowledge, only a couple of articles have been published in the open literature about modeling wire-and-tube condensers in the forced convection regime on the air side. Hoke *et al*. (1997) performed experimental investigations using single-layer wire-and-tube condensers to measure the air-side heat transfer coefficients under forced-convection conditions. They measured the heat transfer coefficient for different angles of attack for two different cases: airflow perpendicular to the tubes and parallel to the wires as well as airflow parallel to the tubes and perpendicular to the wires. Using their experimental results, they developed a model to calculate the air-side heat transfer coefficient. The authors

found that correlations developed by Hilpert (1933) and Žukauskas (1972) for single cylinders overestimated the air-side heat transfer coefficient.

Lee *et al*. (2001) also performed experiments using single-layer sample wire-and-tube condensers to measure the air-side heat transfer coefficient under in the forced convection regime. Based on their experimental results, the authors disagree with the conclusion by Hoke *et al*. (1997) that the heat transfer coefficient correlation developed by Žukauskas (1972) overpredicts the air-side heat transfer coefficient. Using their experimental results, the authors developed correction factors to use with the Žukauskas correlation. With the use of their correction factors, the heat transfer coefficient correlation can be used to model three different airflow configurations—airflow perpendicular to both the tubes and the wires, airflow perpendicular to the tubes and parallel to the wires, and airflow parallel to the tubes and perpendicular to the wires. They define these airflow configurations as all cross, tube cross, and wire cross, respectively.

3.1 Fin Efficiency of Wire-and-Tube Condensers

The fin efficiency is one of the main parameters affecting heat transfer on the air side, so an accurate model is needed to be able to calculate the heat transfer from wire-and-tube condensers accurately. The fin efficiency of a wire can be calculated using the fin efficiency of a thin rod, which is given by the following equation (Myers, 1998):

$$\eta_w = \frac{\tanh(mL)}{mL} \quad \text{where} \quad m = \sqrt{\frac{hp_w}{k_w A_w}} = \sqrt{\frac{4h}{k_w D_w}} \tag{3.1}$$

where L is half the tube spacing in the direction of the wires, h is the heat transfer coefficient, p_w is the perimeter of the wire (πD_w), k_w is the thermal conductivity of the material, and A_w is the cross-sectional area of the wire ($\pi D_w^2/4$). Once the wire efficiency has been calculated, the total surface effectiveness can be calculated according to the following equation:

$$\eta_s = \frac{A_{tube} + \eta_w A_{wire}}{A_{total}} = 1 - (1 - \eta_w)\frac{A_w}{A_{total}} \tag{3.2}$$

3.2 Natural Convection Heat Transfer Model

The heat transfer from the refrigerant to the air can be calculated according to Fourier's law (Bansal and Chin, 2003):

$$q = UA \cdot \Delta T = UA \cdot (T_{ref} - T_{air}) \tag{3.3}$$

where UA is the overall heat transfer conductance and T_{air} is the ambient air temperature. In the model presented in this thesis, UA is, once again, calculated according to Eq. 2.11.

As can be seen in the equations for UA (Eq. 2.11) and the fin efficiency (Eq. 3.1), these two quantities are dependent on the air-side heat transfer coefficient. Therefore, a correlation is needed to calculate the heat transfer coefficient of wire-and-tube condensers undergoing natural convection heat transfer. In typical air-to-refrigerant heat exchangers, radiative heat transfer is dominated by forced convection heat transfer caused by air being blown through by a fan. The radiative component of the total heat transfer can therefore be neglected for modeling purposes. However, in the natural convection regime, the transfer of heat from condensers is due to both

natural convective heat transfer and radiative heat transfer. Therefore, in order to model wire-and-tube condensers under natural convection conditions, both convective heat transfer and radiative heat transfer must be accounted for in the air-side heat transfer coefficient.

As suggested by Tagliafico and Tanda (1997), the air-side heat transfer coefficient can be modeled as the sum of a natural convection heat transfer coefficient and a radiative heat transfer coefficient:

$$h_{air} = h_c + h_r \tag{3.4}$$

Now correlations for each of the individual component heat transfer coefficients are needed.

An empirical correlation can be used to model the natural convection heat transfer coefficient. To the author's knowledge, the correlation developed by Tanda and Tagliafico (1997) is the only natural convection heat transfer coefficient correlation available in the open literature, so it has been implemented in CoilDesigner. Their correlation has the following form:

$$h_c = \frac{Nu \cdot k_{air}}{H} \tag{3.5}$$

where

$$Nu = 0.66\left(\frac{Ra \cdot H}{D_t}\right)^{0.25}\left\{1-\left[1-0.45\left(\frac{D_t}{H}\right)^{0.25}\right]\exp\left(-\frac{s_w}{\varphi}\right)\right\} \tag{3.6}$$

where H is the height of the condenser, the Rayleigh number, Ra, is

$$Ra = \left(\frac{\beta\rho^2 c_p}{\mu k}\right)_{air} g \cdot \left(T_t - T_{air}\right) \cdot H^3 \tag{3.7}$$

and

$$\varphi = \left(\frac{C_1}{H}\right)^{0.4} s_w^{0.9} s_t^{-1.0} + \left(\frac{C_1}{H}\right)^{0.8} \left(\frac{C_2}{T_t - T_{air}}\right)^{0.5} s_w^{-1.5} s_t^{-0.5} \tag{3.8}$$

where C_1=28.2 m, C_2=264 K, and s_t and s_w are the following geometric parameters:

$$s_t = \frac{S_t - D_t}{D_t} \tag{3.9}$$

$$s_w = \frac{S_w - D_w}{D_w} \tag{3.10}$$

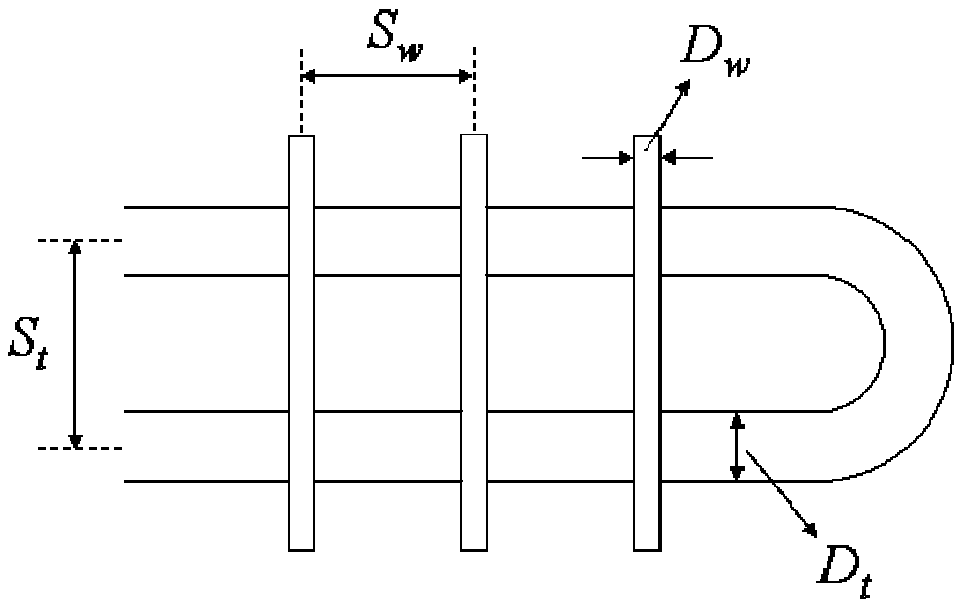

Figure 3-1. Geometric parameters of wire-and-tube condensers

The quantity T_t, used in Eqs. 3.7 and 3.8 above and in Eq. 3.13 below is the temperature of the outside of the tube. It is calculated according to the following equation:

$$T_t = T_{ref} - q \cdot \left(\frac{1}{h_{ref} A_{t,in}} + \frac{R_{thermal}}{A_{t,out}}\right) \tag{3.11}$$

This equation is derived from the fact that, in steady state, the heat transfer from the refrigerant to the air must be equal to the heat transfer from the refrigerant to the outer

surface of the tube. As can be seen in Eq. 3.11, T_t is a function of the heat load of a segment, so it must be guessed initially. As will be explained below, an iterative solution scheme is used to solve the equations in the natural convection model and to calculate the temperature of the tube.

As noted before, Tagliafico and Tanda (1997) also developed a theoretical model to calculate the radiative heat transfer coefficient:

$$h_r = \varepsilon_{app}\sigma\frac{\left(T_{ex}^4 - T_{air}^4\right)}{\left(T_{ex} - T_{air}\right)} \tag{3.12}$$

where ε_{app} is the apparent thermal emittance, which is a function of the thermal emittance of the heat exchanger surface as well as of geometric parameters such as the tube and wire diameters and the tube and wire pitches. Bansal and Chin (2003) found good agreement with experimental results by setting ε_{app} equal to 0.88. σ is the Stefan-Boltzmann constant, $5.67\text{x}10^{-8}$ W/(K^4 m^2). T_{ex} is the mean surface temperature of the heat exchanger, which can be calculated according to the following equation:

$$T_{ex} = \frac{T_t + GP\cdot\eta_w\cdot\left(T_t - T_{air}\right) + GP\cdot T_{air}}{1 + GP} \tag{3.13}$$

where GP is a geometric parameter dependent on the tube and wire pitches and diameters, given by the following equation:

$$GP = 2\left(\frac{S_t}{D_t}\right)\cdot\left(\frac{D_w}{S_w}\right) \tag{3.14}$$

The radiative heat transfer coefficient is a function of the wire efficiency, η_w, because the mean external temperature is a function of the wire efficiency. The wire efficiency, in turn, is a function of the heat transfer coefficient, as shown in Eq. 3.1.

Because of this interdependence, an iterative procedure must be used to calculate the heat transfer coefficients, the wire efficiency, and the external temperature of the heat exchanger. Bansal and Chin (2003) presented an iterative scheme for these calculations, shown in Figure 3-2, which has been implemented in CoilDesigner.

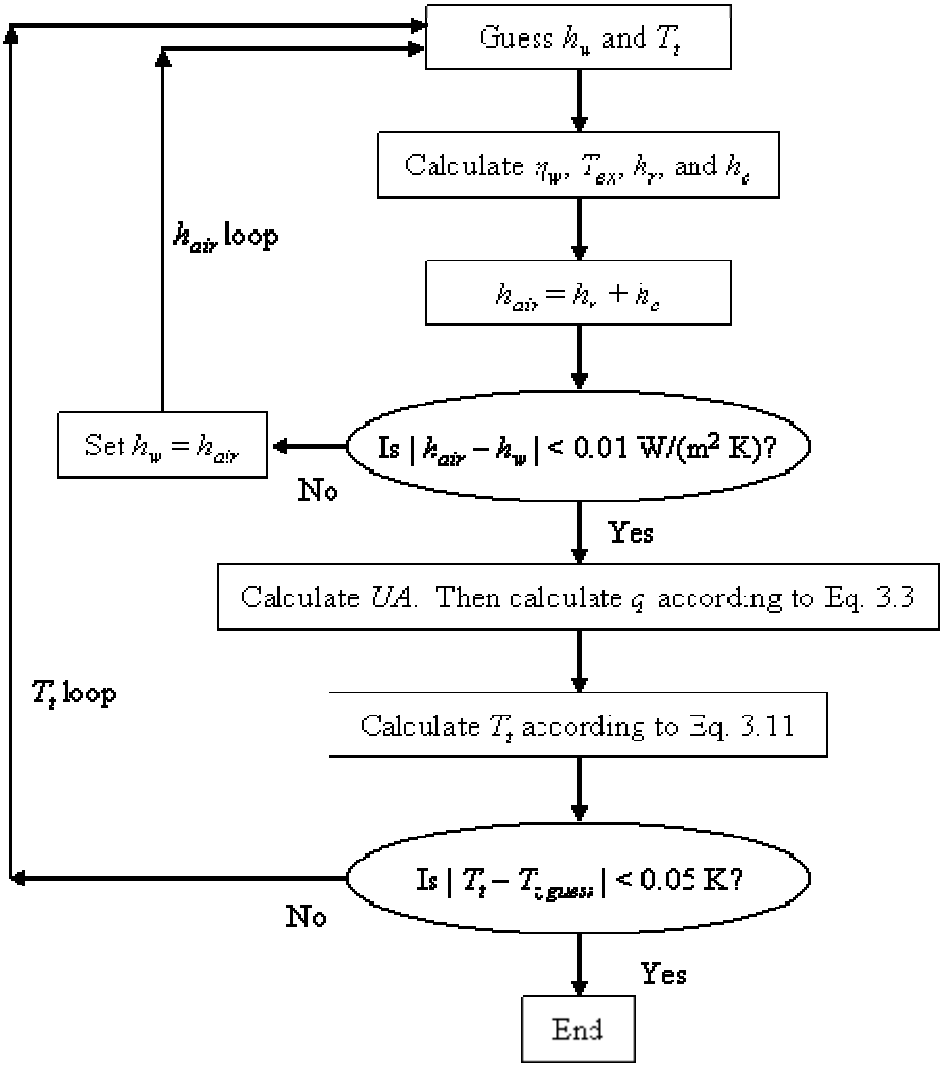

Figure 3-2. Flow chart for iterative scheme to calculate air-side heat transfer coefficient and heat load for natural convection wire-and-tube condensers (adapted from Bansal and Chin, 2003)

3.3 Forced Convection Heat Transfer Model

Many wire-and-tube condensers in modern refrigerators employ forced convection heat transfer on the air side. As noted before, these condensers typically consist of a long tube bent into several rows and columns to form a tube bundle. A fan is used to circulate air through the condenser. This type of condenser is very similar to round tube plate fin (RTPF) heat exchangers except that wires are used as the extended surface instead of plate fins. Because of this similarity, the heat transfer from wire-and-tube condensers can be modeled in the same way as for RTPF heat exchangers. In other words, the ε-NTU method described in Section 2.2 can be used to calculate the heat transfer from the refrigerant to the air. The only modification that needs to be made is in the calculation of the air-side heat transfer coefficient. Correlations developed specifically for wire-and-tube condensers undergoing forced convection heat transfer are necessary. For this reason, the heat transfer coefficient correlations developed by Hoke *et al*. (1997) and Lee *et al*. (2001) for wire-and-tube condensers have both been included in CoilDesigner.

Hoke *et al*. (1997) developed two heat transfer coefficient correlations—one for airflow perpendicular to the tubes and parallel to the wires and one for airflow parallel to the tubes and perpendicular to the wires. The heat transfer coefficient for airflow perpendicular to the tubes and parallel to the wires has been implemented in CoilDesigner. Their equation for the Nusselt number is

$$Nu_w = C \cdot Re_w^n \left\{1 - C_2 \exp\left(-C_3 S_w^*\right)\right\} \tag{3.15}$$

where Re_w is the Reynolds number based on the wire diameter, and S_w^* is the dimensionless wire spacing using the wire diameter as the characteristic length:

$$S_w^* = \frac{S_w}{D_w} \tag{3.16}$$

The constants in Eq. 3.15 are given by the following equations:

$$C = 0.259 - 0.232\cos(\alpha)\exp\left(-0.00289\alpha^2\right) \tag{3.17}$$

$$n = 0.55 + 0.269\cos(\alpha)\exp\left(-0.00597\alpha^2\right) \tag{3.18}$$

where α is the angle of attack of the airflow, $C_2 = 100$, and $C_3 = 2.32$. Currently, CoilDesigner only has the capability of modeling airflow at an attack angle of 0^o, in which case Eq. 3.17 and 3.18 reduce to $C = 0.027$ and $n = 0.819$.

As mentioned before, Lee *et al*. (2001) developed correction factors to use with the Žukauskas (1972) heat transfer coefficient correlation for a single cylinder. With the use of these correction factors, the heat transfer coefficient correlation can be used to model three different airflow configurations—all cross, tube cross, and wire cross. Their correlation has been implemented in CoilDesigner for the cases of all cross (i.e. perpendicular to the tubes and wires) and tube cross (i.e. perpendicular to the tubes and parallel to the wires). Their correlation has the following form

$$h = \frac{K}{\eta_s A_{total}} \tag{3.19}$$

where η_s is the surface effectiveness as shown in Eq. 3.2. The value K is the air-side thermal conductance, which is essentially calculated as a weighted combination of the heat transfer coefficients for the tubes and for the wires. The process for calculating K is as follows. First, a heat transfer coefficient, denoted h_Z, is calculated for both the tubes and for the wires using the Žukauskas correlation:

$$h_{Z,t} = C \cdot Re_t^m \cdot Pr_{air}^{0.37} \cdot \frac{k_{air}}{D_t} \tag{3.20}$$

$$h_{Z,w} = C \cdot Re_w^m \cdot Pr_{air}^{0.37} \cdot \frac{k_{air}}{D_w} \tag{3.21}$$

The constants *C* and *m* are dependent on the Reynolds number and are provided in Table 3-1.

Table 3-1. Constants *C* and *m* used to calculate the Žukauskas heat transfer coefficient

Reynolds Number	*C*	*m*
1 - 40	0.75	0.4
40 - 1000	0.52	0.5
1000 - $2x10^5$	0.26	0.6
$2x10^5$ - $2x10^6$	0.023	0.8

Once the individual heat transfer coefficients for the tubes and the wires have been calculated, *K* is calculated for the case of airflow perpendicular to the tubes and the wires (all-cross) according to the following equation

$$K = F_c \cdot \left(h_{Z,t} A_t + \eta_w h_{Z,w} A_w\right) \tag{3.22}$$

For the case of airflow perpendicular to the tubes and parallel to the wires (tube-cross), *K* is calculated according to the following equation

$$K = F_c h_{Z,t} A_t + \eta_w F_p h_{Z,w} A_w \tag{3.23}$$

In both of the preceding equations, the wire efficiency, η_w, is calculated according to Eq. 3.1, using $h_{Z,w}$ as the heat transfer coefficient. The factors F_c and F_p are the correction factors developed by Lee *et al*. based on if the airflow is cross flow or parallel flow, respectively. For cross flow, they found good agreement with experimental results by setting the correction factor, F_c, equal to a constant:

$$F_c = 1.3 \tag{3.24}$$

For parallel flow, they derived the following equation to calculate the correction factor:

$$F_p = 0.063 \cdot Re^{0.37} \tag{3.25}$$

Modeling of forced convection wire-and-tube condensers has been performed and compared with experimental data as part of a validation study. This modeling work is detailed in Section 7.2. As part of the study, the predictions of the correlations developed by Hoke *et al*. and by Lee *et al*. were compared. In agreement with Lee *et al*., the correlation developed by Hoke *et al*. was found to underpredict the air-side heat transfer coefficient. Thus, while both correlations have been included in CoilDesigner, the correlation developed by Lee *et al*. is recommended.

Chapter 4 Flat Tube Heat Exchanger Model

Flat tube heat exchangers, such as those depicted in Figure 4-1 and Figure 4-2, are often used for automotive applications such as radiators and charge air coolers. This fluid-to-air type of heat exchanger usually contains a fluid such as a water/glycol mixture or some other coolant inside the tubes. The use of flat tubes allows for better airflow over the tubes compared to round tube plate fin (RTPF) heat exchangers. Achieving better airflow can help to reduce the fan power consumption as well as the resistance to heat transfer. In order to model flat tube heat exchangers in CoilDesigner, a new solver has been created that can account for the unique geometric and fluid flow characteristics of flat tube heat exchangers.

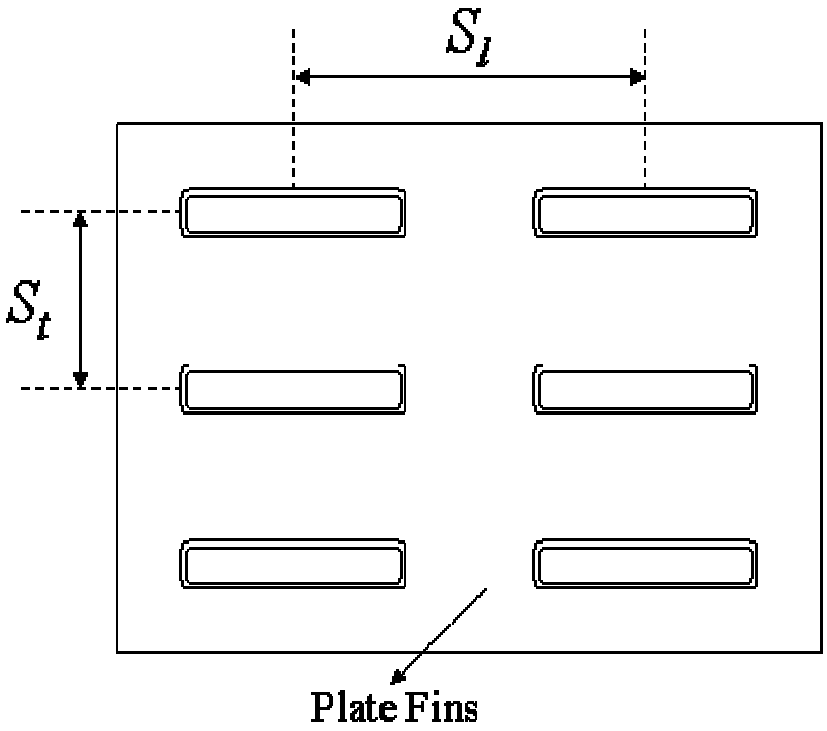

Figure 4-1. Flat tube heat exchanger with plate fins

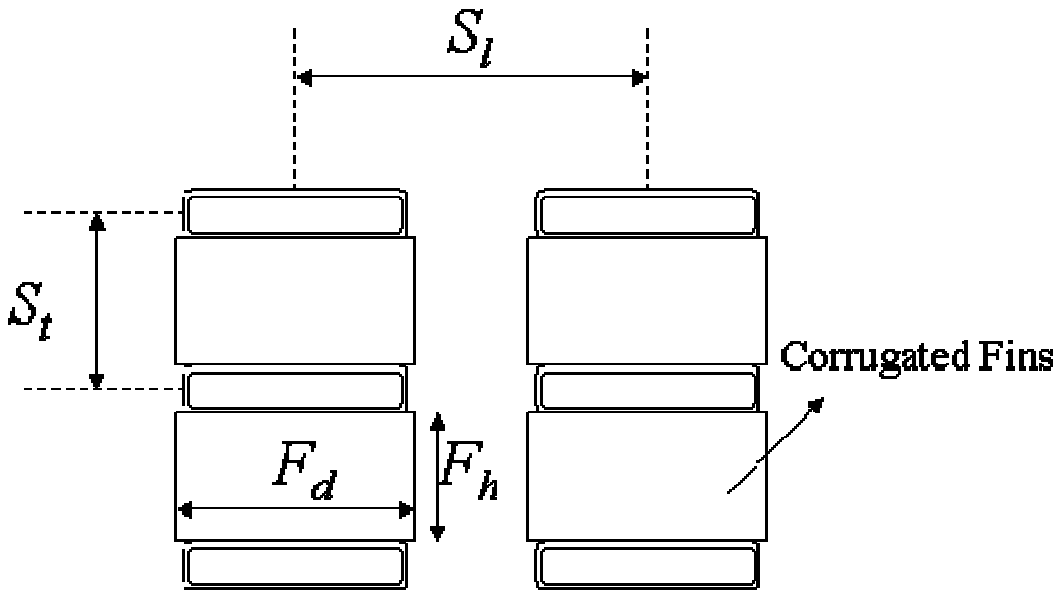

Figure 4-2. Flat tube heat exchanger with corrugated fins

The flat tube heat exchanger model must be able to model the following different options for fluid flow configuration, fin type, and tube configuration:

- Fluid flow configurations
    - Serpentine
    - Parallel
- Fin types
    - Plate fins
    - Corrugated fins
- Tube configurations
    - Inline
    - Staggered

Changes have been made to CoilDesigner to allow for all of these different options. The changes as well as the modeling equations for the heat transfer and pressure drop are detailed in the following sections.

4.1 Fluid-Side Modeling

On the fluid side, the heat transfer coefficients and pressure drop are calculated with correlations that were already included in CoilDesigner (Jiang, 2003). The hydraulic diameter of the flat tube is used in these correlations instead of the inner diameter of a round tube:

$$D_h = 4 \cdot \frac{A_c}{P_{wet}} = 4 \cdot \frac{T_{h,in} \cdot T_{w,in}}{2 \cdot \left(T_{h,in} + T_{w,in}\right)} \tag{4.1}$$

where A_c is the cross-sectional area of the inside of the tube and P_{wet} is the wetted perimeter of the inside of the tube. $T_{h,in}$ and $T_{w,in}$ are the tube inner height and the tube inner width, respectively, as shown in Figure 4-3.

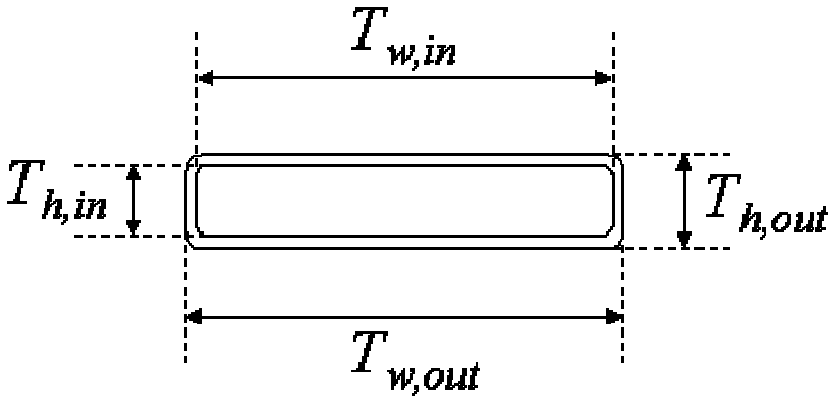

Figure 4-3. Geometric parameters of flat tubes

Flat tube heat exchangers can have two different fluid flow configurations. The first is serpentine flow, which is similar to most RTPF heat exchangers and is shown in Figure 4-4. Typically in this type of configuration, the fluid flows through each tube of the heat exchanger in series, and a tube is connected to the next tube in the tube circuitry by a bend.

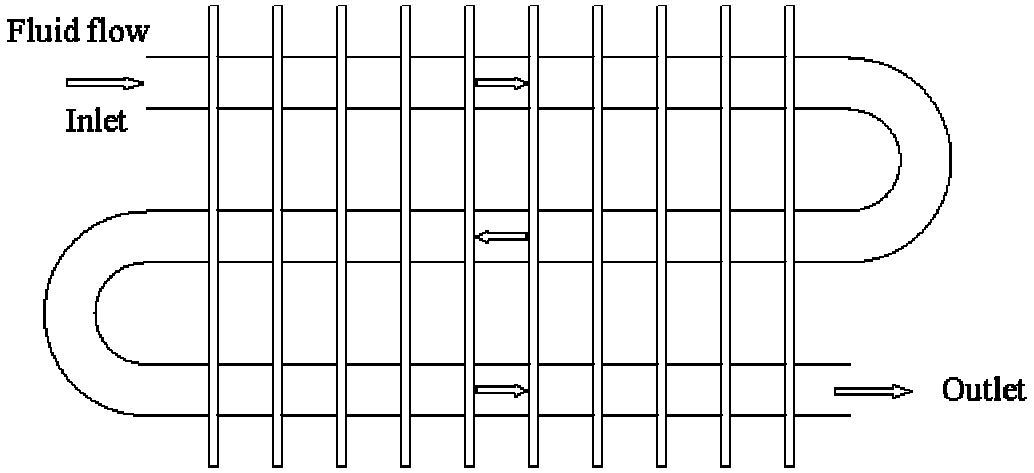

Figure 4-4. Flat tube heat exchanger with serpentine refrigerant flow (airflow into the page)

The second type of fluid flow configuration is parallel flow, which is the type of flow employed in most microchannel heat exchangers and is shown in Figure 4-5. In this type of configuration, the fluid splits into several streams inside a header and then flows through multiple tubes in parallel. The fluid enters the tubes from one header and then is combined at the other end of the tubes in another header before flowing on to either the next header or to the heat exchanger outlet.

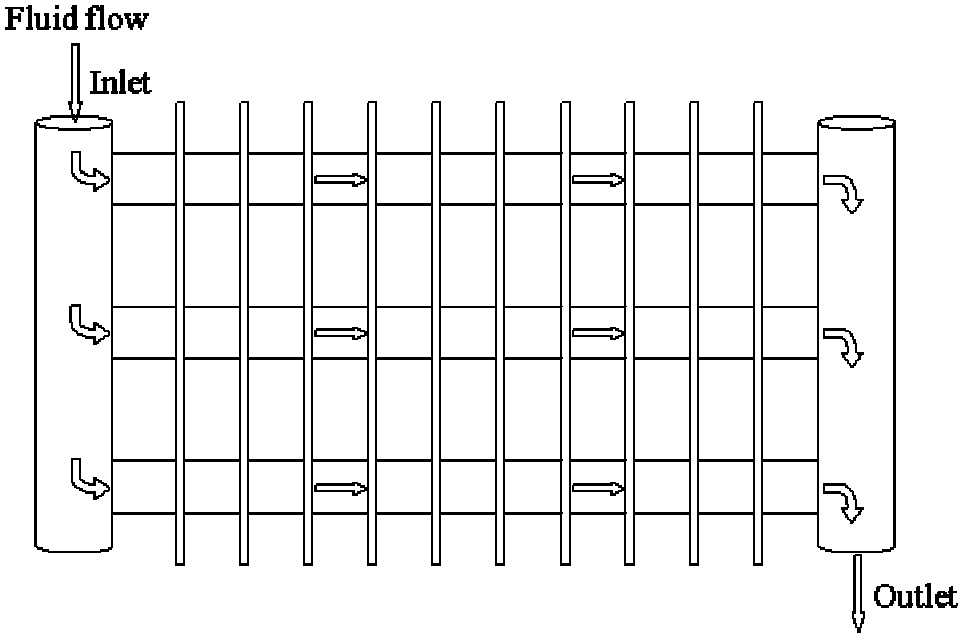

Figure 4-5. Flat tube heat exchanger with parallel refrigerant flow (airflow into the page)

To simulate this type of flow configuration, the fluid flow from upstream tubes to downstream tubes must be modeled. In order to do this, the concept of a junction, which was defined by Jiang (2003), is used. A junction is defined as the intersection where two or more tubes are joined together. In heat exchangers with parallel flow, a header is considered to be a junction. In steady state, the mass flow rate into a junction from all of the upstream tubes must equal the mass flow rate flowing out of the junction through all of the downstream tubes. This is expressed by the following equation

$$\sum_i \dot{m}_{i,in} = \sum_i \dot{m}_{i,out} \tag{4.2}$$

where *i* represents a tube. The total energy flow entering a junction from all of the upstream tubes is also equal to the energy flow leaving the junction through the downstream tubes:

$$\sum_i \dot{m}_{i,in} h_{i,in} = \sum_i \dot{m}_{i,out} h_{i,out} \tag{4.3}$$

The enthalpy of the fluid entering each tube downstream of a junction is calculated as the weighted average of the enthalpy of the fluid entering the junction from the upstream tubes:

$$h_{i,out} = \frac{\sum_i \dot{m}_{i,in} h_{i,in}}{\sum_i \dot{m}_{i,out}} \tag{4.4}$$

4.2 Heat Transfer Between Refrigerant and Air

As in the other CoilDesigner models, each tube is divided into multiple segments, and the energy and hydraulic calculations are performed for each segment.

Also, as in the CoilDesigner models for heat exchanger types that employ forced convection on the air side, the ε-NTU method for cross-flow configuration with one fluid mixed and the other fluid unmixed is used to calculate the heat load of each segment (Kays and London, 1984). Once again, the air side is modeled as an unmixed fluid and the refrigerant side is modeled as a mixed fluid. Thus, the heat transfer between the refrigerant and the air for flat tube heat exchangers is modeled using the same ε-NTU equations given in Chapter 2.

4.3 Air-Side Modeling

4.3.1 Fin Types for Flat Tube Heat Exchangers

Flat tube heat exchangers can have either plate fins, like those in RTPF heat exchangers, or corrugated fins, which are the same as those found in microchannel heat exchangers. Both types of fin have been included in the flat tube model in CoilDesigner. Details about their implementation are included below.

Plate Fins

Flat tube heat exchangers with plate fins are very similar to round tube plate fin heat exchangers, except for the shape of the tube. After an extensive literature search, the only correlations that could be found for the air-side heat transfer coefficient and pressure drop were those developed by Achaichia and Cowell (1988) for flat tube heat exchangers with louvered plate fins. Louvered fins are often used because they enhance the air-side heat transfer. The louvers disrupt the path of the

airflow, thereby increasing the turbulence of the air and impeding the formation of the thermal boundary layer, which in turn increases the heat transfer.

No other air-side correlations could be found for flat tube heat exchangers, even for flat plate fins because this type of fin is apparently rarely used. However, if modeling flat plate fins is necessary, the air-side heat transfer coefficient and pressure drop correlations by Kim *et al*. (1999) developed for RTPF heat exchangers could be used with correction factors. The tube outer height, $T_{h,out}$, can be set as the outer diameter for the purposes of the air-side correlations because this is the amount of the air stream blocked by the tube. Obviously the airflow around flat tubes and the turbulence induced will be different than for round tubes. However, the heat transfer coefficient and pressure drop should exhibit the same trends with respect to changes in parameters such as air velocity, fin spacing, and tube spacing. Therefore, with suitable correction factors, the correlations by Kim *et al*. should predict reasonably accurate results for the heat transfer coefficient and pressure drop.

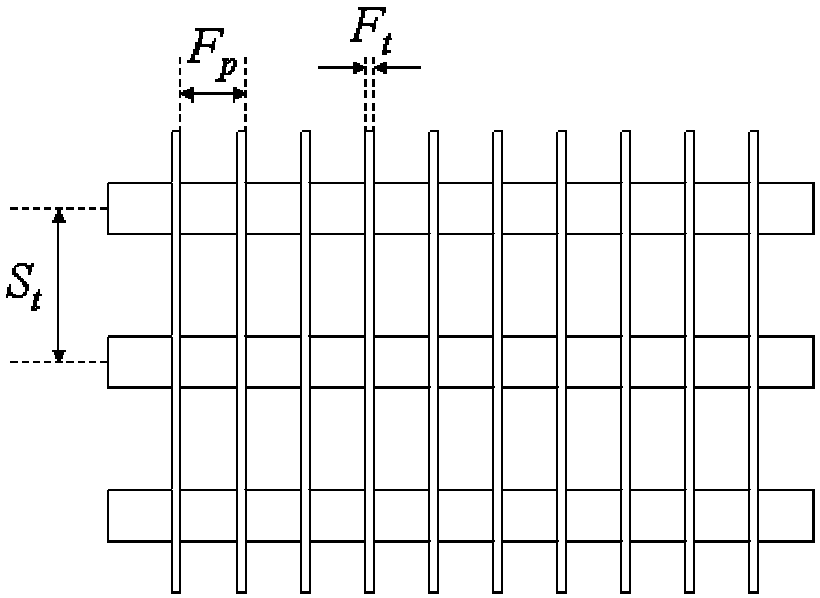

Figure 4-6. Flat tube heat exchanger with plate fins (airflow into the page)

Since the air-side heat transfer coefficient and pressure drop correlations by Achaichia and Cowell (1988) were the only ones that could be found for flat tube plate fin heat exchangers, they have been implemented in CoilDesigner and are described below.

Achaichia and Cowell found that they could obtain better correlations using the Reynolds number based on the louver pitch, shown in Figure 4-7, rather than the air-side hydraulic diameter. Therefore, their correlations use the Reynolds number based on the louver pitch:

$$Re_{Lp} = \frac{L_p G}{\mu_{air}} \tag{4.5}$$

where the mass flux, G, is the mass flux through the minimum free flow area:

$$G = \rho_{air} \cdot v_{max} \tag{4.6}$$

where v_{max} is the maximum velocity in the core of the heat exchanger:

$$v_{max} = v_{air,in} \cdot \frac{A_{frontal}}{A_{min}} \tag{4.7}$$

where $A_{frontal}$ is the frontal face area of the heat exchanger and A_{min} is the minimum free flow area for the air to pass through.

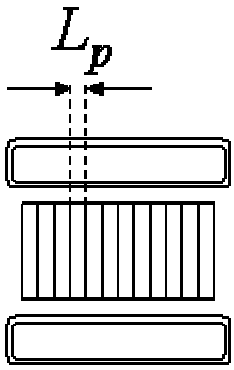

Figure 4-7. Diagram showing the definition of louver pitch

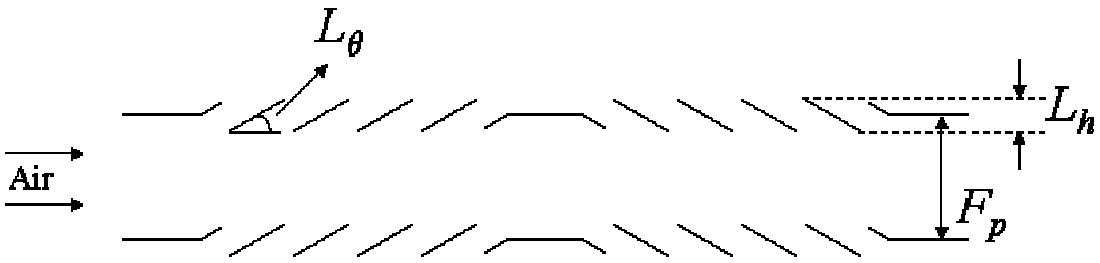

Figure 4-8. Diagram showing the definition of louver angle and louver height

Achaichia and Cowell developed correlations for the Stanton number. If the Reynolds number based on the louver pitch is between 150 and 3000, the Stanton number can be calculated according to the following equation:

$$St = 1.54 \cdot Re_{Lp}^{-0.57} \left(\frac{F_p}{L_p} \right)^{-0.19} \left(\frac{S_t}{L_p} \right)^{-0.11} \left(\frac{L_h}{L_p} \right)^{0.15} \tag{4.8}$$

where the louver height, L_h, is given by the following equation:

$$L_h = L_p \cdot \sin\left(L_\theta\right) \tag{4.9}$$

If the Reynolds number is between 75 and 150, the Stanton number can instead be calculated according to the following equation:

$$St = 1.554 \cdot \frac{\beta}{L_\theta} Re_{Lp}^{-0.59} \left(\frac{S_t}{L_p} \right)^{-0.09} \left(\frac{F_p}{L_p} \right)^{-0.04} \tag{4.10}$$

where β is a mean fluid flow angle which the authors have defined by the following equation:

$$\beta = 0.936 - \frac{243}{Re_{Lp}} - 1.76 \cdot \frac{F_p}{L_p} + 0.995 \cdot L_\theta \tag{4.11}$$

Once the Stanton number has been calculated, the heat transfer coefficient is calculated according to the following equation:

$$h = St \cdot G \cdot c_{p,air} \tag{4.12}$$

Based on their experimental measurements, Achaichia and Cowell (1988) also created correlations to calculate the Fanning friction factor. If the Reynolds number is between 150 and 3000, then the Fanning friction factor is calculated as follows:

$$f = 0.895 \cdot f_A^{1.07} F_p^{-0.22} L_p^{0.25} S_t^{0.26} L_h^{0.33} \tag{4.13}$$

where

$$f_A = 596 \cdot Re_{Lp}^{[0.318 \cdot (\ln Re) - 2.25]} \tag{4.14}$$

If the Reynolds number is less than 150, Achaichia and Cowell found that the friction factor was best represented by the following equation:

$$f = 10.4 \cdot Re_{Lp}^{-1.17} F_p^{0.05} L_p^{1.24} L_h^{0.25} S_t^{0.83} \tag{4.15}$$

Once the Fanning friction factor has been calculated, the air-side pressure drop is calculated according to the following equation:

$$\Delta P = f \cdot \frac{A_{total}}{A_{min}} \cdot \frac{G^2}{2\rho_{air}} \tag{4.16}$$

where A_{total} is the total surface area of the tubes and the fins.

Corrugated Fins

Corrugated fins, also known as serpentine fins, are depicted in Figure 4-9 and Figure 4-10. This type of fin is used often in flat tube heat exchangers as well as in microchannel heat exchangers. Flat tube and microchannel heat exchangers with corrugated fins actually have the same geometry on the air side. Therefore, correlations developed for either type of heat exchanger can be used.

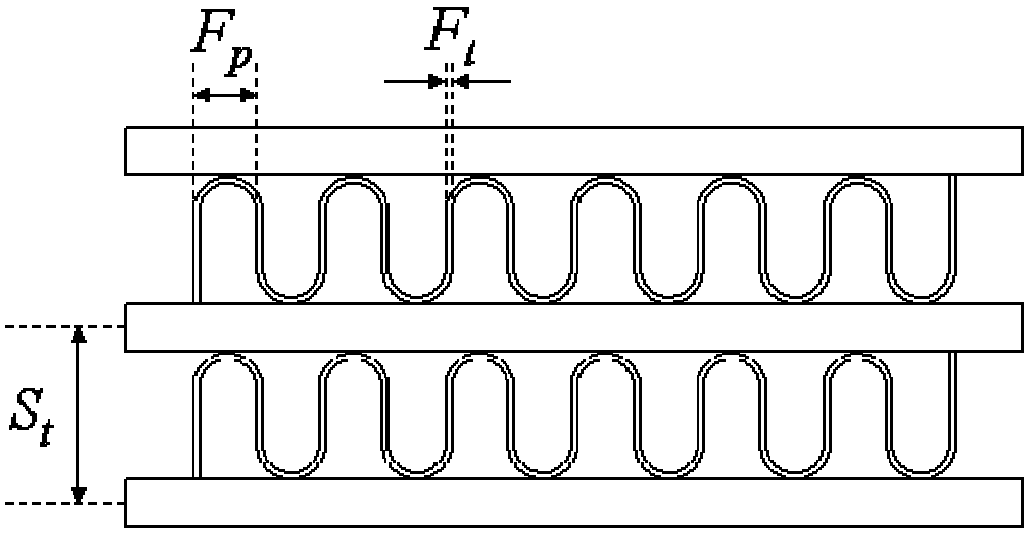

Figure 4-9. Flat tube heat exchanger with corrugated fins (airflow into the page)

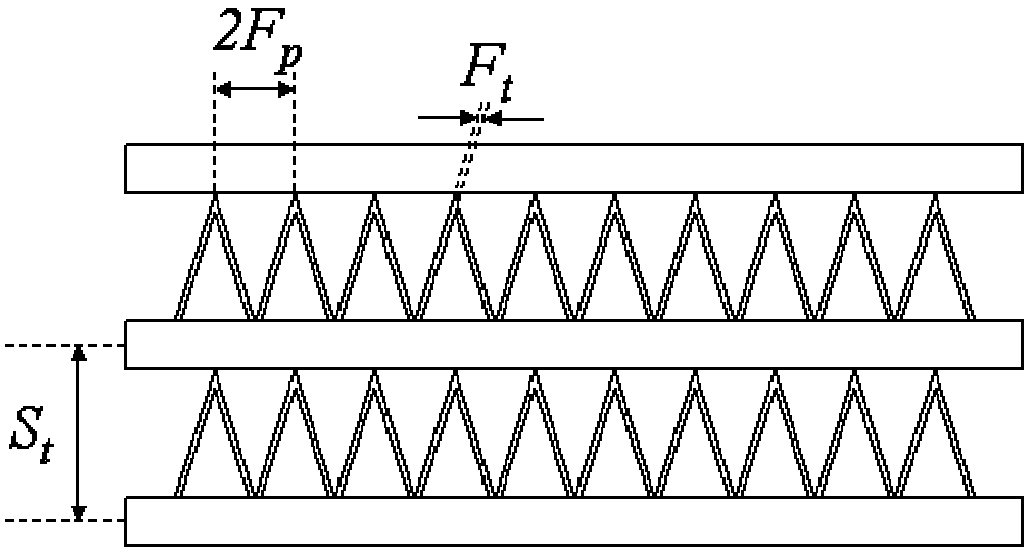

Figure 4-10. Flat tube heat exchanger with triangular corrugated fins (airflow into the page)

Multiple heat transfer coefficient and pressure drop correlations have been developed for corrugated fins over the past couple of decades. As a part of this research on flat tube heat exchangers and as a part of the research on microchannel heat exchanger simulation, a comprehensive literature search has been performed for air-side heat transfer coefficient and pressure drop correlations for corrugated fins.

The heat transfer coefficient correlations are typically provided in the form of the Colburn *j* factor, which can then be used to calculate the heat transfer coefficient:

$$h = \frac{j \cdot G \cdot c_{p,air}}{Pr_{air}^{2/3}} = St \cdot G \cdot c_{p,air} \tag{4.17}$$

where the Stanton number is equal to $j/Pr^{2/3}$. The pressure drop correlations are typically provided in the form of the Fanning friction factor, *f*, described above.

Correlations to calculate the *j* and *f* factors for plain corrugated fins were developed by Heun and Dunn (1996) using data provided by Kays and London (1984). These correlations have been included in CoilDesigner and are detailed in the Appendix.

The majority of correlations have been developed for louvered corrugated fins because this is the most common type of fin used in flat tube and microchannel heat exchangers. Several investigators, including Davenport (1983), Rugh *et al*. (1992), Sahnoun and Webb (1992), Sunden and Svantesson (1992), Dillen and Webb (1994), and Chang and Wang (1996) developed correlations for the Colburn *j* factor and the friction factor, *f*, for louvered fins. Chang and Wang (1997) compiled experimental data measured by the some of the previous authors as well as by other investigators and developed a database with 768 heat transfer coefficient measurements and 1109 friction factor measurement from a total of 91 sample heat exchangers. Chang and Wang then used this database to develop a new generalized correlation for the *j* factor. Chang *et al*. (2000) used the database to develop a generalized correlation for the friction factor, *f*. Because their heat transfer coefficient and friction factor correlations were developed using such an extensive set of data, they are applicable to a rather wide range of geometries and flow conditions. These correlations have been

found to provide very accurate results and have become accepted standard correlations used in industry. Therefore, the Chang and Wang (1997) and the Chang *et al*. (2000) correlations have been included in CoilDesigner and are detailed in the Appendix.

4.3.2 Tube Configurations for Flat Tube Heat Exchangers

Similar to RTPF heat exchangers, flat tube heat exchangers can have both inline tube configurations, as shown before in Figure 4-1, and staggered tube configurations, as shown below in Figure 4-11.

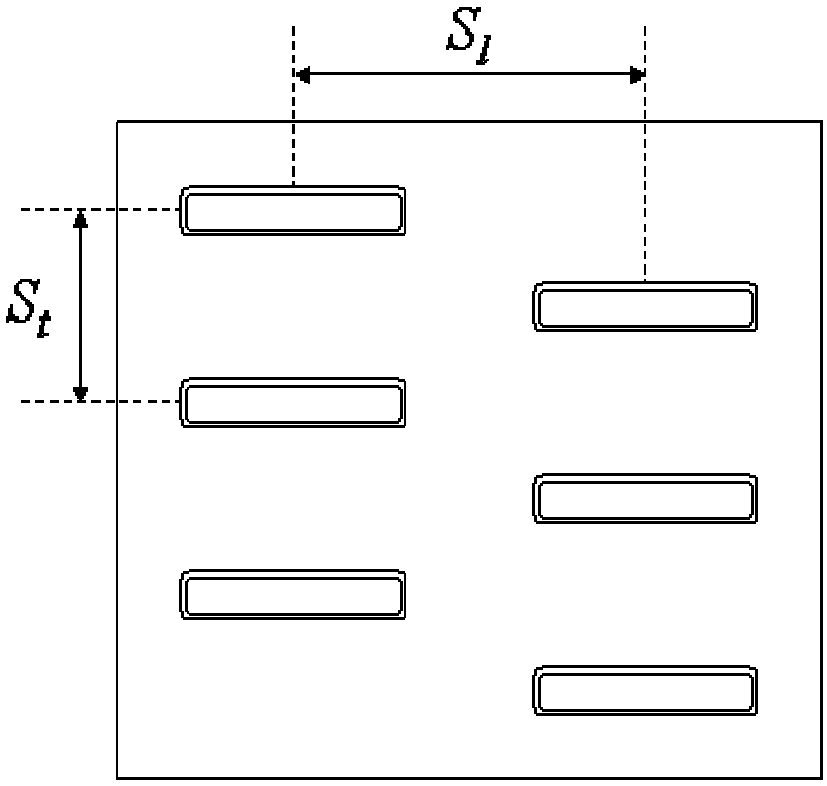

Figure 4-11. Flat tube plate fin heat exchanger with staggered tube configuration

The mass and energy conservation between the neighboring segments are modeled in the same manner as for round tube plate fin heat exchangers (Jiang,

2003). For inline tube arrangements, the inlet air properties of a segment are set equal to the outlet air properties of the corresponding segment of the tube upstream in the airflow:

$$\dot{m}_{air,k} = \dot{m}_{air,i} \tag{4.18}$$

$$\dot{m}_{air,k} \cdot h_{air,k,in} = \dot{m}_{air,i} \cdot h_{air,i,out} \tag{4.19}$$

The subscripts *i* and *k* are defined in Figure 4-12. For staggered tube arrangements, the inlet air properties of a segment are set equal to average of the outlet properties of the two previous upstream segments:

$$\dot{m}_{air,k} = 0.5 \cdot \left(\dot{m}_{air,i} + \dot{m}_{air,j} \right) \tag{4.20}$$

$$\dot{m}_{air,k} \cdot h_{air,k,in} = 0.5 \cdot \left(\dot{m}_{air,i} \cdot h_{air,i,out} + \dot{m}_{air,j} \cdot h_{air,j,out} \right) \tag{4.21}$$

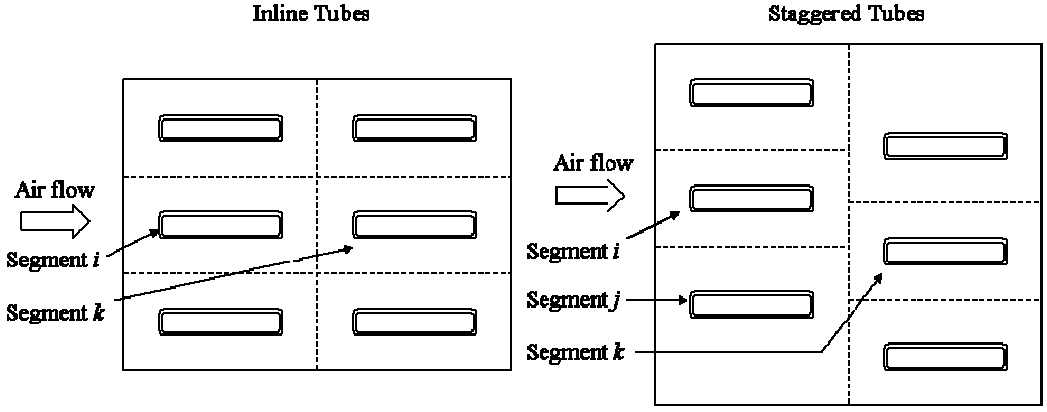

Figure 4-12. Air-side mass and energy flow from one column of tubes to the next

Chapter 5 Void Fraction Models and Charge Calculation

One important feature of heat exchanger software modeling tools is the ability to predict the mass of refrigerant, or the refrigerant charge, in a heat exchanger. The calculation of refrigerant charge is very important in vapor compression system simulation for charge management. In single-phase flow, the charge can be calculated in a straightforward manner by multiplying the density of the refrigerant times the volume. Previously the charge in a segment was calculated in CoilDesigner similarly, by multiplying the average density of the two-phase refrigerant by the volume of the segment. However, in an effort to improve the charge prediction capabilities of CoilDesigner, the void fraction is now used to calculate the charge.

The void fraction is defined as the fraction of a tube occupied by vapor:

$$\alpha = \frac{A_{vap}}{A_c} \tag{5.1}$$

where A_{vap} is the cross-sectional area occupied by vapor and A_c is the total cross-sectional area of the tube:

$$A_c = A_{vap} + A_{liq} \tag{5.2}$$

In the case of annular flow in a round tube, Eq. 5.1 reduces to

$$\alpha = \left(1 - \frac{\delta}{R}\right)^2 \tag{5.3}$$

where δ is the liquid film thickness and R is the radius of the tube.

The charge in a segment is calculated according to the following equation:

$$Charge_{segment}\left[kg\right] = \left(1-\alpha\right)\cdot \rho_{liq} \cdot L_{seg} \cdot A_c + \alpha \cdot \rho_{vap} \cdot L_{seg} \cdot A_c \tag{5.4}$$

By accounting for the actual volume of a segment occupied by each phase of the refrigerant this equation results in a more accurate calculation of the charge. The charge in an entire heat exchanger is then calculated by summing the charge in each segment of each tube:

$$Charge_{total}[kg] = \sum_{tube} \sum_{segment} Charge_{segment} \tag{5.5}$$

Accurate void fraction models are needed to predict refrigerant charge. However, analytical void fraction models typically are not very accurate (Harms *et al*., 2003). Therefore, many investigators over the past few decades have developed empirical models to calculate the void fraction in two-phase flow. An extensive literature search of these void fraction models was performed, and multiple models have been included in CoilDesigner. A majority of the models have been developed for annular two-phase flow because this is the dominant flow regime in evaporators and condensers. A rather large number of models has been included because the predictions of different void fraction models can vary greatly (Rice, 1987). Moreover, obtaining experimental charge data can be difficult, making it difficult to compare model predictions with the charge of actual heat exchangers. Therefore, selecting certain "better" correlations to include in CoilDesigner was not very practical. All of the void fraction models that were researched have been included in CoilDesigner, and it is left up to the user to decide which models predict charge better. However, future studies should be performed with experimental charge data to determine which void fraction models do a better job at predicting charge so that certain models can be recommended.

Void fraction models can be classified into four main categories—homogeneous, slip-ratio-correlated, Lockhart-Martinelli parameter correlated, and mass-flux dependent (Rice, 1987). Each type of model is detailed in the following sections and correlations based on each type of model are given.

5.1 Types of Void Fraction Model

5.1.1 Homogeneous Void Fraction Model

The homogeneous void fraction models ideal two-phase flow. This model is the most simplistic and assumes two-phase flow to be a homogeneous mixture with the liquid and the vapor traveling at the same velocity. The void fraction in this case can be calculated according to the following equation:

$$\alpha = \frac{1}{1+\left(\frac{1-x}{x}\right)\frac{\rho_{vap}}{\rho_{liq}}} \tag{5.6}$$

Some models simply multiply a constant times the homogeneous void fraction. Examples of this are models by Armand (1946) and Ali *et al*. (1993), which can be used for microchannel tubes and are detailed in the Appendix.

5.1.2 Slip-Ratio-Correlated Void Fraction Models

Slip-ratio-correlated void fraction models build on the homogeneous model, but the assumption that the liquid and vapor phases travel at the same velocity is abandoned. The liquid and vapor phases are modeled as two separate streams, each with its own velocity. The slip ratio is defined as the ratio of the vapor velocity to the liquid velocity:

$$S = \frac{v_{vap}}{v_{liq}} \tag{5.7}$$

For slip-ratio-correlated models, investigators develop a method to calculate the slip ratio. The void fraction is then calculated by modifying the homogeneous void fraction model as follows to in order to account for the slip ratio:

$$\alpha = \frac{1}{1 + \left(\frac{1-x}{x}\right)\frac{\rho_{vap}}{\rho_{liq}} \cdot S} \tag{5.8}$$

Several investigators have developed empirical slip-ratio-correlated void fraction models, and they were all developed for annular two-phase flow. Models by Thom (1964), Zivi (1964), Smith (1969), and Rigot (1973) have been included in CoilDesigner and are detailed in the Appendix.

5.1.3 Void Fraction Models Correlated With Lockhart-Martinelli Parameter

Another group of void fraction models avoids the homogeneous void fraction model altogether, and instead correlates the void fraction with the Lockhart-Martinelli parameter. These models are developed for stratified flow. The Lockhart-Martinelli parameter, which is discussed in further detail in Section 6.6, is calculated according to the following equation:

$$X_{tt} = \left(\frac{1-x}{x}\right)^{0.9} \sqrt{\left(\frac{\mu_{liq}}{\mu_{vap}}\right)^{0.2} \cdot \frac{\rho_{vap}}{\rho_{liq}}} \tag{5.9}$$

Lockhart and Martinelli (1949) and Baroczy (1966) presented void fraction data as a function of X_{tt}. Other investigators have since created correlations with their data.

These correlations have been implemented in CoilDesigner and are included in the Appendix.

5.1.4 Mass-Flux-Dependent Void Fraction Models

Mass-flux-dependent void fraction models are typically correlated to the mass flux through the use of the Reynolds number. Tandon *et al*. (1985) developed an analytical model for annular flow. Premoli (1971), Yashar *et al*. (2001), and Harms *et al*. (2003) all developed empirical models for annular flow. Hughmark (1962) developed an empirical void fraction model for the bubbly flow regime in vertical upward flow, but found that the correlation worked well for other flow regimes and in horizontal tubes. Rouhani and Axelsson (1970) developed an empirical model that can be used for all of the different boiling regions. These void fraction models are all detailed in the Appendix.

5.2 Comparison of Void Fraction Models

A comparison of the charge predictions based on the different void fraction models was performed. A round tube plate fin condenser was modeled in CoilDesigner with an inlet quality of 0.99 and an outlet quality of about 0.06 in order to cover almost the entire quality range. The charge was calculated with each built-in void fraction model that was developed for round tubes. The results are presented in Figure 5-1 and show that there is a wide variation in the predictions of the different models.

Obtaining experimental data regarding refrigerant charge inventory in heat exchangers is difficult. Therefore, it is difficult to ascertain which void fraction models provide accurate predictions. For this reason, all of the correlations that were researched have been included in CoilDesigner for the user to choose from. However, as stated before, experimental charge data should be obtained in the future and studies should be performed to compare the predictions of void fraction models with actual charge inventory.

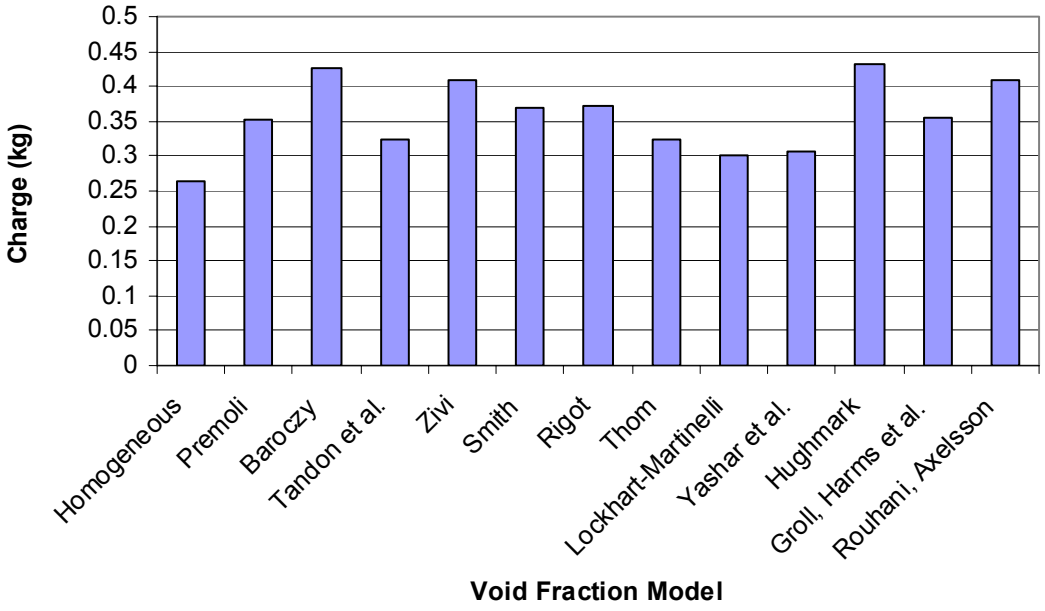

Figure 5-1. Comparison of charge predictions based on different void fraction models

Chapter 6 Modeling of Effects of Oil in Heat Exchangers

In vapor compression systems used in HVAC&R systems, oil is required as a lubricant and sealant in the compressor. Some of this oil becomes entrained in the working fluid and is thus circulated along with the refrigerant through the different components of a vapor compression system. The presence of oil in the working fluid can have a significant impact on the heat transfer and pressure drop through cycle components. In order to be able to model HVAC&R systems more accurately, and to be able to optimize them for variables such as lubricant selection and refrigerant and oil charge, it is necessary to be able to model the effects of oil on heat transfer and pressure drop in evaporators and condensers as well as oil retention in these components.

The presence of oil changes the thermodynamic and physical properties of the working fluid. Instead of calculating properties such as temperature, density, viscosity, and surface tension with property calls to Refprop, as is done for pure refrigerants, methods are necessary to account for the changes due to the presence of oil. The evaporation and condensation processes are also different when oil is present. As opposed to evaporation and condensation processes for pure refrigerants, which occur at a constant temperature, refrigerant-oil mixtures behave similar to zeotropic mixtures because there is a temperature glide as the mixture quality changes. This alters the way the heat load must be calculated because there is a sensible heat load component in addition to the normal latent heat load component. Correlations are also necessary for modeling the heat transfer coefficient and pressure drop with oil present.

The additional capabilities necessary to model the presence of oil have been included in CoilDesigner. This modeling work was performed with Lorenzo Cremaschi, a former Ph.D. student in the Center for Environmental Energy Engineering at the University of Maryland, to simulate heat exchanger performance with oil entrainment (2004). As a part of this modeling work, equations have been added to calculate refrigerant-oil mixture properties. In addition, heat transfer coefficient and pressure drop correlations have been implemented that account for the effects of oil. To calculate the heat load during evaporation and condensation, the method developed by Thome (1995) has been included. Models for calculating oil retention in evaporators and condensers have also been added. After making all of these changes, simulations were performed, and the results have been compared with experimental results obtained by Cremaschi during his experiments regarding oil retention in vapor compression systems. The details of the modeling work are provided in this chapter. In Chapter 7, a comparison between modeled and experimental results is included.

6.1 Oil Mass Fraction and Two-Phase Refrigerant-Oil Mixture Quality

The local properties of the liquid refrigerant-oil mixture, including the mixture temperature, are highly dependent on the concentration of oil in the mixture. However, the concentration of oil in the liquid refrigerant-oil mixture actually changes throughout a heat exchanger. This is because the oil circulating through vapor compression systems does not evaporate, so the oil remains concentrated chiefly in the liquid phase refrigerant. Therefore, the concentration of oil in the liquid

refrigerant is dependent on the quality of the refrigerant-oil mixture. As the mixture quality increases (i.e. more refrigerant evaporates) the concentration of oil in the remaining liquid refrigerant increases, so it must be calculated in each segment.

In order to calculate the local oil concentration, a baseline oil concentration for a system must be defined at a point where the refrigerant-oil mixture is completely in the liquid phase. This occurs between the condenser outlet and the expansion device. The absolute oil mass fraction for a system is defined at this location according to the following equation:

$$\omega_0 = \frac{\dot{m}_{oil}}{\dot{m}_{oil} + \dot{m}_{ref}} \tag{6.1}$$

As the refrigerant-oil mixture travels through the evaporator and condenser, the quality of the mixture will change as refrigerant evaporates or condenses. Analogous to the calculation of the quality of a refrigerant in the two-phase region, the local quality of the refrigerant-oil mixture can be calculated as follows

$$x_{mix} = \frac{\dot{m}_{ref,vap}}{\dot{m}_{ref,vap} + \dot{m}_{ref,liq} + \dot{m}_{oil}} \tag{6.2}$$

Once the absolute oil mass fraction and the local mixture quality have been calculated, the local oil mass fraction can be calculated. Using the conservation of mass and assuming all of the oil remains in the liquid phase, the local oil mass fraction is given by the following equation

$$\omega_{local} = \frac{\omega_0}{1 - x_{mix}} \tag{6.3}$$

Because it is assumed that the oil remains in the liquid phase, there exists a maximum possible quality for the refrigerant-oil mixture, which is less than 1:

$$x_{mix,\max} = \frac{\dot{m}_{ref,vap}}{\dot{m}_{ref,vap} + \dot{m}_{oil}} = 1 - \omega_0 \tag{6.4}$$

If, during an evaporation process, the refrigerant-oil mixture reaches $x_{mix,max}$, the temperature of the mixture can increase without the quality of the mixture increasing. Thus, because the refrigerant has evaporated out of the liquid refrigerant-oil mixture, the refrigerant-oil mixture enters the so-called superheating region without all of the mixture being in the vapor phase.

6.2 Bubble Point Temperature Calculation

In order to be able to model heat transfer and the physical properties of refrigerant-oil mixtures in heat exchangers, a method to calculate the temperature of such mixtures is necessary. Refrigerant-oil mixtures behave in a manner similar to zeotropic refrigerants because, at a constant saturation pressure, the temperature increases as the quality increases, resulting in a temperature glide during the evaporation and condensation processes. The temperature difference between a refrigerant-oil mixture and the saturation temperature of the pure refrigerant, as a function of quality, is depicted in Figure 6-1. The temperature of such mixtures cannot be evaluated directly with Refprop. However, in Thome's (1995) work developing a "thermodynamic approach" to model refrigerant-oil mixtures, he included a method that can be used to calculate the bubble point temperature of different refrigerant-oil mixtures using an empirical equation. This method has been included in CoilDesigner to calculate the temperature of refrigerant-oil mixtures and is described in the following paragraphs.

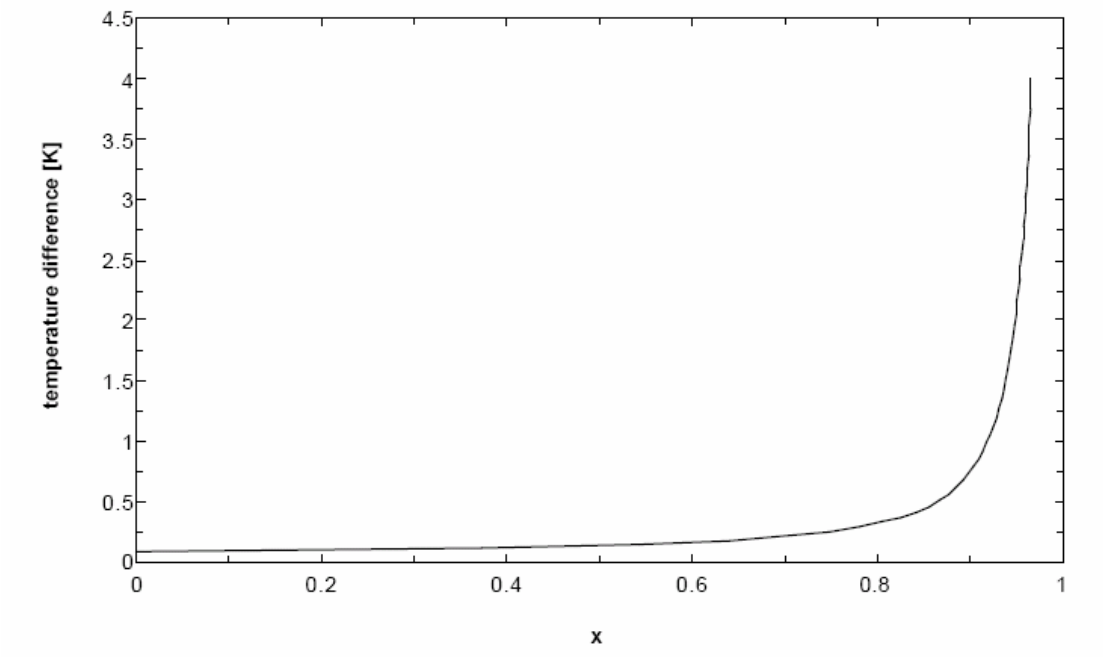

Figure 6-1. Difference between refrigerant-oil mixture bubble point temperature and refrigerant saturation temperature, as a function of quality (From Shen and Groll, 2003, p. 6)

Thome (1995) adopted an equation developed by Takaishi and Oguchi (1987) to calculate the bubble point temperature of a refrigerant-oil mixture based on the saturation pressure and the local oil mass fraction:

$$T_{bub} = \frac{A(\omega_{local})}{\ln P_{sat} - B(\omega_{local})} \tag{6.5}$$

where ω_{local} is the oil mass fraction in the liquid in a segment and P_{sat} is the local saturation pressure in MPa. The constants $A(\omega_{local})$ and $B(\omega_{local})$ can be calculated according to the following equations

$$A(\omega_{local}) = a_0 + a_1\omega_{local} + a_2\omega_{local}^3 + a_3\omega_{local}^5 + a_4\omega_{local}^7 \tag{6.6}$$

$$B(\omega_{local}) = b_0 + b_1\omega_{local} + b_2\omega_{local}^3 + b_3\omega_{local}^5 + b_4\omega_{local}^7 \tag{6.7}$$

Takaishi and Oguchi fitted the constants in Eqs. 6.6 and 6.7 for an R-22/synthetic alkyl benzene oil mixture. The values of the constants $a_1 - a_4$ and $b_1 - b_4$ are provided in the following table:

Table 6-1. Empirical constants used in Eqs. 6.6 and 6.7 to calculate bubble point temperature of refrigerant-oil mixtures

a_1	182.52	b_1	-0.72212
a_2	-724.21	b_2	2.3914
a_3	3868.0	b_3	-13.779
a_4	-5268.9	b_4	17.066

Thome (1995) extended Eqs. 6.6 and 6.7 to other refrigerant-oil mixtures beyond R-22/synthetic alkyl benzene oil by suggesting that only a_0 and b_0 must be adjusted. He reasoned that the values of the other constants can be considered to remain constant for different refrigerant-oil pairs and saturation pressures because the vapor pressure of the oil is negligible. Thome suggested that the values of the constants a_0 and b_0 can be correlated depending on the specific pure refrigerant and the saturation pressure. They are calculated using the following procedure:

- Calculate the saturation temperatures for the pure refrigerant at two different pressures, one just below the local saturation pressure and one just above
- Set ω_{local} equal to zero and evaluate Eq. 6.5 with the two different pairs of T_{sat} and P_{sat}
- Solve the resulting system of two equations for the two unknowns, a_0 and b_0

This method provides a relatively simple, yet accurate way to calculate the bubble point temperature of different refrigerant-oil mixtures during evaporation and condensation processes.

6.3 Heat Load Calculation and the Heat Release Enthalpy Curve

As in the CoilDesigner solver for pure refrigerants, the ε-NTU method is used to calculate the heat load in a segment with a refrigerant-oil mixture. For pure refrigerant undergoing an evaporation or condensation process, the heat load causes boiling or condensing, resulting in an increase or decrease in the enthalpy and the quality with no change in temperature. The change in enthalpy is given by the equation

$$dh = h_{LV} \cdot dx \tag{6.8}$$

On the other hand, for a refrigerant-oil mixture, the heat load causes evaporation or condensation as well as a change in the temperature of the refrigerant-oil mixture. The change in enthalpy in a segment consists of three components (Thome, 1995):

- Latent heat due to evaporation or condensation
- Sensible heat due to the change in bubble point temperature of the liquid-phase refrigerant-oil mixture
- Sensible heat due to the change in bubble point temperature of the vapor-phase refrigerant

The change in enthalpy in this case is given by the following equation, known as the heat release enthalpy curve:

$$dh = h_{LV} \cdot dx_{mix} + \left(1 - x_{mix}\right) \cdot c_{p,mix} \cdot dT_{bub} + x_{mix} \cdot c_{p,ref,vapor} \cdot dT_{bub} \tag{6.9}$$

Once the heat load of a segment is calculated using the ε-NTU method, the resulting change in quality, dx_{mix}, and the resulting change in the bubble point temperature, dT_{bub}, must be calculated. Essentially this means dividing the heat load

into sensible and latent components. This is necessary so that the outlet temperature and quality of the refrigerant-oil mixture can be passed as inputs to the next segment.

As described in Section 6.2, the bubble point temperature is dependent on the quality of the refrigerant-oil mixture. Thus, all three terms on the right-hand side of Eq. 6.9 are functions of dx_{mix}. The result is that an iterative numerical scheme must be used to calculate the correct values of dx_{mix} and dT_{bub}. Ridders' method (Press, 1992) has been implemented to calculate the change in quality that will result in the correct outlet temperature and the correct heat load.

In the iterative method employed, an outlet quality is guessed. For an evaporation process, the guessed outlet quality is between the inlet quality and $x_{mix,max}$. For a condensation process, the guessed outlet quality is between the inlet quality and zero. Based on the guessed outlet quality, the outlet oil mass fraction, ω_{local}, is calculated according to Eq. 6.3, and then the outlet temperature is calculated according to Eq. 6.5.

Once an outlet quality has been guessed and the outlet temperature has been calculated, the change in quality and temperature through the segment, dx_{mix} and dT_{bub}, can be calculated. The change in enthalpy can then be calculated according to Eq. 6.9. This change in enthalpy is then compared to the heat load calculated using the ε-NTU method. If these two heat load values do not agree within a specified tolerance, Ridders' method guesses another value for the outlet quality and the steps above are repeated.

6.4 Calculation of Refrigerant-Oil Mixture Properties

The thermodynamic and transport properties of refrigerant-oil mixtures are very important for calculating heat transfer and pressure drop, so methods for calculating these properties were necessary. Shen and Groll (2003) provided a comprehensive review of the literature regarding refrigerant-oil mixture property calculations. They suggested methods for calculating properties such as density, viscosity, and specific heat of refrigerant-oil mixtures. These methods have been included in CoilDesigner to calculate mixture properties and are summarized below. Unless specified otherwise, the properties of oil used in the following equations were obtained from manufacturing data. The properties of liquid and vapor refrigerant are calculated by making function calls to Refprop using P_{sat} and T_{bub} as the inputs.

- **Liquid mixture density**

  The density of the mixture of liquid refrigerant and oil is calculated using the method given by Jensen and Jackman (1984):

$$\frac{1}{\rho_{mix}} = \frac{\omega_{local}}{\rho_{oil}} + \frac{1-\omega_{local}}{\rho_{ref,liq}} \tag{6.10}$$

- **Liquid mixture viscosity**

  The viscosity of the mixture of liquid refrigerant and oil is calculated using the method provided by Yokozeki (1994):

$$\ln \mu_{mix} = \sum_i \xi_i \cdot \ln \mu_i = \xi_{ref,liq} \cdot \ln \mu_{ref,liq} + \xi_{oil} \cdot \ln \mu_{oil} \tag{6.11}$$

  where ξ_i is the Yokozeki factor

$$\xi_i = \frac{W_i^k \Psi_i}{\sum_j W_j^k \Psi_j} \tag{6.12}$$

and W_i and Ψ_i are the molecular mass and the mole fraction, respectively, of component i. The exponent k is an empirical constant that is specific to different refrigerant-oil pairs. However, Yokozeki found that setting $k = 0.58$ provided accurate results for most refrigerant-oil pairs. The mole fraction of the oil can be obtained from the equation

$$\Psi_{oil} = \frac{\omega_{local}\left(\frac{W_{ref}}{W_{oil}}\right)}{1-\omega_{local}+\omega_{local}\left(\frac{W_{ref}}{W_{oil}}\right)} \tag{6.13}$$

- **Liquid mixture surface tension**

  The surface tension of the mixture of liquid refrigerant and oil is also calculated according to the method provided by Jensen and Jackman (1984):

$$\sigma_{mix} = \sigma_{ref,liq} + \left(\sigma_{oil} - \sigma_{ref,liq}\right)\sqrt{\omega_{local}} \tag{6.14}$$

- **Liquid mixture thermal conductivity**

  The thermal conductivity of the mixture of liquid refrigerant and oil is calculated according to the method provided by Filippov and Novoselova (1955):

$$k_{mix} = k_{ref,liq}\left(1-\omega_{local}\right) + k_{oil}\omega_{local} - 0.72\left(k_{oil} - k_{ref,liq}\right)\left(1-\omega_{local}\right)\omega_{local} \tag{6.15}$$

- **Liquid mixture specific heat**

  The specific heat of the mixture of liquid refrigerant and oil is calculated according to the method provided by Jensen and Jackman (1984):

$$c_{p,mix} = \omega_{local}c_{p,oil} + \left(1-\omega_{local}\right)c_{p,ref,liq} \tag{6.16}$$

  The specific heat of the oil is calculated according to the following equation recommended by Thome (1995)

$$c_{p,oil} = 4.186\left(\frac{0.338 + 0.00045 \cdot \left(1.8 \cdot T\left[^{\circ}\mathrm{C}\right] + 32\right)}{\sqrt{s_g}}\right) \tag{6.17}$$

where s_g is the specific gravity of the oil, $s_g = \rho_{oil}/\rho_{water}$, at 15.6°C.

- **Liquid and vapor phase Reynolds numbers**

  The Reynolds numbers for the liquid and vapor phases are calculated using the quality of the refrigerant-oil mixture, x_{mix}:

$$Re_{liq} = \frac{G_{total} \cdot \left(1 - x_{mix}\right) \cdot D}{\mu_{mix,liq}} \tag{6.18}$$

$$Re_{vap} = \frac{G_{total} \cdot x_{mix} \cdot D}{\mu_{ref,vap}} \tag{6.19}$$

6.5 Heat Transfer Coefficient Correlations for Refrigerant-Oil Mixture

6.5.1 Heat Transfer Coefficient for Evaporation

As mentioned before, the ε-NTU method was used to calculate the heat load for refrigerant-oil mixtures. This method requires the calculation of a heat transfer coefficient on the refrigerant side. Thus, in order to be able to model refrigerant-oil mixtures accurately, correlations that account for the presence of oil are needed.

While some previous investigators have used mixture properties directly in correlations developed for pure refrigerants to predict the heat transfer coefficient of refrigerant-oil mixtures, other investigators have created semi-empirical heat transfer coefficient correlations based on pure refrigerant properties (Shen and Groll, 2003). However, as discussed by Shen and Groll (2003), these correlations do not generally provide very accurate predictions because either they were developed for pure

refrigerants or because they use pure refrigerant properties. Therefore, they do not capture the true behavior of refrigerant-oil mixtures during evaporation.

Chaddock and Mathur (1980) developed the only semi-empirical correlation that is based on refrigerant-oil mixture properties. They developed their correlation using experimental results for flow boiling of R-22/Suniso 3 GS oil inside a smooth tube. Shen and Groll (2003) recommended extending the semi-empirical correlation developed by Chaddock and Mathur to other refrigerant-oil mixture pairs. Therefore, the correlation, which has the following form, has been implemented in CoilDesigner:

$$\frac{h_{two-phase,mix}}{h_{liq}} = c\left(\frac{1}{X_{tt}}\right)^{n} \tag{6.20}$$

where X_{tt} is the Lockhart-Martinelli parameter of the refrigerant-oil mixture. The calculation of the Lockhart-Martinelli parameter is described in Section 6.6. The constants c and n are semi-empirical constants that depend on the oil mass fraction and are given in Table 6-2. The liquid heat transfer coefficient is calculated using the Dittus-Boelter correlation (1930) with the refrigerant-oil mixture properties:

$$\begin{aligned} h_{liq} &= 0.023\left(\frac{k_{ref,liq}}{D}\right) Re_{mix,liq}^{0.8} \cdot Pr_{mix,liq}^{0.4} \\ &= 0.023\left(\frac{k_{ref,liq}}{D}\right)\left(\frac{G\cdot(1-x_{mix})\cdot D}{\mu_{mix,liq}}\right)^{0.8}\left(\frac{c_{p,ref,liq}\cdot\mu_{mix,liq}}{k_{ref,liq}}\right)^{0.4} \end{aligned} \tag{6.21}$$

where G is the total mass flux of the refrigerant and oil. The correlation was developed by Chaddock and Mathur for mass fluxes varying from 149.0 to 908.5 kg/(m^2 s), heat fluxes varying from 7.73 to 40.54 kW/m^2, and vapor quality varying from 0.0 to 1.0.

Table 6-2. Coefficients c and n as a function of the oil mass fraction in the correlation developed by Chaddock and Mathur (1980) for the heat transfer coefficient of refrigerant-oil mixtures

Oil Mass Fraction (wt. %)	*c*	*n*
0.0	3.90	0.62
1.0	4.72	0.59
2.9	4.36	0.60
5.7	4.97	0.59

6.5.2 Heat Transfer Coefficients for Condensation

The heat transfer coefficient for single-phase refrigerant-oil mixtures in the subcooled region can be calculated using traditional single-phase correlations such as the Dittus-Boelter (1930) and Gnielinski (1976) correlations with the refrigerant-oil mixture properties.

As with evaporating heat transfer coefficients, previous researchers have modeled two-phase convective condensing heat transfer coefficients of refrigerant-oil mixtures using pure refrigerant correlations with the mixture properties or by developing semi-empirical correlations based on either pure refrigerant properties or refrigerant-oil mixture properties (Shen and Groll, 2003). The presence of oil has been shown to have less of an adverse effect on convective condensation compared to convective evaporation. Therefore, efforts to calculate the condensation heat transfer coefficient using existing correlations with refrigerant-oil mixture properties have met with greater success than for evaporation. Shah's condensation correlation (1979) using mixture properties has been shown to predict the heat transfer coefficient accurately (Shen and Groll, 2003), so it has been implemented in CoilDesigner. Shah's method first calculates the liquid-phase heat transfer coefficient using the

Dittus-Boelter correlation, given in Eq. 6.21, and then multiplies this quantity by the following two-phase multiplier:

$$C = 1 + \frac{3.8}{P_r^{0.38}} \left(\frac{x_{mix}}{1 - x_{mix}} \right)^{0.76} \tag{6.22}$$

where P_r is the reduced pressure of the refrigerant (P/P_{crit}).

6.6 Pressure Drop Correlation for Two-Phase Refrigerant-Oil Mixture

The presence of oil can reduce the frictional pressure drop as the refrigerant flows through the tubes of a heat exchanger (Shen and Groll, 2003). The main reason for this phenomenon is that the oil increases the viscosity of the fluid, which can cause a transition to laminar flow from what would normally be turbulent flow. This can be illustrated with the equation for the liquid Reynolds number, Eq. 6.18, in which increasing the viscosity decreases the Reynolds number. The liquid Reynolds number can drop below the transition point between laminar and turbulent, especially at higher qualities, since it is proportional to $1–x_{mix}$.

The Lockhart-Martinelli correlation accounts for the flow state (laminar or turbulent) when calculating the pressure drop. Thus, the influence of oil on the flow state and hence on the pressure drop can be captured by using the Lockhart-Martinelli correlation with mixture properties (Shen and Groll, 2003). Therefore, it has been recommended by Shen and Groll and implemented in CoilDesigner to predict the pressure drop of refrigerant-oil mixtures. The pressure drop is calculated according to the following procedure. First, the Lockhart-Martinelli parameter is calculated according to the following equation:

$$X_{tt} = \left[\frac{-\Delta P_{mix,liq}}{-\Delta P_{vap}} \right]^{0.5} \tag{6.23}$$

where the liquid-phase and vapor-phase frictional pressure drops are calculated according to the following two equations:

$$\Delta P_{mix,liq} = f_{mix,liq} \frac{L_{seg} G^2 \left(1 - x_{mix}\right)^2}{2D\rho_{mix,liq}} \tag{6.24}$$

$$\Delta P_{vap} = f_{vap} \frac{L_{seg} G^2 x_{mix}^2}{2D\rho_{vap}} \tag{6.25}$$

where L_{seg} is the length of the segment. The friction factor for each phase is calculated according to the following equations, depending on whether the flow is laminar or turbulent:

$$f_k = \frac{16}{Re_k} \text{ for } Re_k < 2000 \tag{6.26}$$

$$f_k = \frac{0.046}{Re_k^{0.2}} \text{ for } Re_k > 2000 \tag{6.27}$$

where the liquid and vapor Reynolds numbers are calculated as in Eqs. 6.18 and 6.19. When both the liquid phase and the vapor phase are turbulent, the Lockhart-Martinelli parameter reduces to the following rather well-known equation:

$$X_{tt} = \left(\frac{1 - x_{mix}}{x_{mix}} \right)^{0.9} \sqrt{\left(\frac{\mu_{mix,liq}}{\mu_{vap}} \right)^{0.2} \cdot \frac{\rho_{vap}}{\rho_{mix,liq}}} \tag{6.28}$$

After the Lockhart-Martinelli parameter has been calculated, the two-phase multiplier for each phase must be calculated according to the following equations:

$$\phi_{mix,liq}^2 = 1 + \frac{C}{X_{tt}} + \frac{1}{X_{tt}^2} \tag{6.29}$$

$$\phi_{vap}^2 = 1 + CX_{tt} + X_{tt}^2 \tag{6.30}$$

where the constant C is determined by the flow states of the vapor and the liquid, as shown in Table 6-3.

Table 6-3. Constant *C* used to calculate the two-phase multipliers used in the Lockhart-Martinelli correlation

Liquid Flow State	Vapor Flow State	*C*
Laminar	Laminar	5
Laminar	Turbulent	10
Turbulent	Laminar	12
Turbulent	Turbulent	20

The two-phase frictional pressure drop is then calculated as the maximum of the pressure drop multiplied by the two-phase multiplier for each phase:

$$\Delta P_{frictional} = Max\left(\Delta P_{mix,liq} \cdot \phi_{mix,liq}^2;\ \Delta P_{vap} \cdot \phi_{vap}^2\right) \tag{6.31}$$

6.7 Oil Retention and Void Fraction Models

One of the motivations for modeling oil in heat exchangers is to model the oil retention for purposes of oil charge management. In order to calculate the oil retention, the void fraction of the two-phase refrigerant-oil mixture must be calculated. The fraction of a segment occupied by liquid is equal to $(1 - \alpha)$, and the fraction of the liquid mixture comprised of oil is ω_{local}. Therefore, the oil retention in a segment can be calculated using a fairly simple modification to Eq. 5.4, the equation for calculating the charge in a segment:

$$ORM_{segment}[kg] = \omega_{local} \cdot V_{segment} \cdot (1-\alpha) \cdot \rho_{mix.liq} \tag{6.32}$$

The total oil retention in an entire heat exchanger is then calculated by summing up the oil retention in each segment of every tube:

$$ORM_{total}[kg] = \sum_{tube} \sum_{segment} ORM_{segment} \tag{6.33}$$

Several void fraction models, such as those by Lockhart-Martinelli (1949), Hughmark (1962), and Premoli *et al*. (1971), have been recommended in the recent literature for the purposes of calculating the void fraction of refrigerant-oil mixtures (Shen and Groll, 2003). In order to use these void fraction models for refrigerant-oil mixtures, the liquid properties such as density are simply replaced with the mixture properties. All of these void fraction models are included in the Appendix. They were all tested with experimental data, and the Premoli void fraction model was found to provide the most accurate results.

Chapter 7 Validation and Optimization Studies

7.1 Validation of Microchannel Heat Exchanger Model

A study was performed to determine the accuracy of the microchannel heat exchanger model. The model was validated with experimental data from 8 microchannel condensers using the refrigerant R-134a. Seven of the heat exchangers comprised of 48 tubes, with the refrigerant making a first pass through 32 tubes and a second pass through 16 tubes. The other heat exchanger comprised of 24 tubes, with the refrigerant making a first pass through 18 tubes and a second pass through 6 tubes. The fins used were louvered, corrugated fins. The geometric parameters of the heat exchangers are provided in Table 7-1. All of the heat exchangers used in the validation had a tube height of 1.9 mm and a fin thickness of 0.114 mm. The experimental data was measured for varying air and refrigerant flow rates and varying inlet conditions. Results from a total of 35 tests were used in the model validation.

Table 7-1. Geometric parameters of the microchannel heat exchangers used for validation

No. of Tubes	Hydraulic Diameter (mm)	Tube Depth (mm)	Tube Length (mm)	Tube Pitch (mm)	Fin Density (fpi)	Fin Depth (mm)	Fin Height (mm)	Louver Length (mm)	Louver Pitch (mm)	No. Data Points
48	0.775	18.77	479.6	10.16	19.6	18.8	7.9	6.6	1.4	4
48	0.775	18.77	479.6	10.16	11.8	21.1	7.9	6.6	1.4	4
48	0.775	18.77	479.6	10.16	19.6	21.1	7.9	6.6	1.4	4
48	0.775	18.77	479.6	10.16	23.6	21.1	7.9	6.6	1.4	4
48	0.771	13.54	479.6	10.16	19.9	15.9	12.7	10.9	1.14	5
48	0.771	13.54	479.6	10.16	19.9	15.9	10.8	9.5	1.4	5
48	0.771	13.54	479.6	10.16	20	15.9	10.0	8.7	1.4	5
24	0.775	18.77	1069	10.48	24	21.1	7.92	6.6	1.4	4

For the air-side heat transfer coefficient and pressure drop calculations, correlations developed specifically for microchannel or flat tube heat exchangers with louvered fins were necessary. The correlations presented by Chang and Wang (1997)

and Chang *et al*. (2000) were used for the air side Colburn *j* factor and the fraction factor, *f*. These correlations are detailed in the Appendix. On the refrigerant side, the Gnielinski correlation (1976) was used for the calculation of single-phase heat transfer coefficients. The correlation developed by Dobson and Chato (1998) for heat transfer during condensation was used in the two-phase region. Good results were obtained using this correlation with a correction factor of 1.5. For the refrigerant-side pressure drop calculations, the correlation developed by Churchill (Chisholm, 1983) was used in the single-phase region, and the correlation developed by Jung and Radermacher (1989) was used for the two-phase region.

The results of the validation are presented in Figure 7-1 and Figure 7-2. As can be seen in Figure 7-1, the heat load was predicted very accurately. 80% of the heat load data points were predicted within 2.25%. All of the heat load data points were predicted with an average error of -0.84%, an average absolute error of 1.6%, and a maximum error of 4.6%. For the refrigerant pressure drop, shown in Figure 7-2, 54.3% of the data points were predicted within 25%, and the average error, average absolute error, and maximum error were -12.1%, 25.9%, and 62.8%, respectively. The refrigerant pressure drop was generally underpredicted. This could be due in part to the fact that the pressure drop through the inlet tube to the heat exchanger was not modeled.

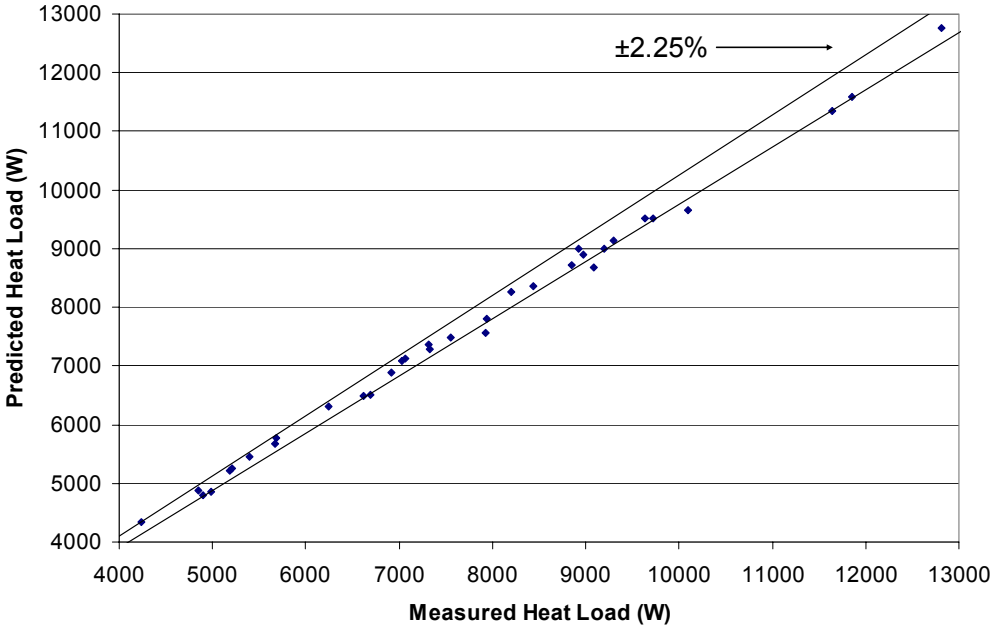

Figure 7-1. Predicted heat load vs. experimentally measured heat load of microchannel heat exchangers used for validation

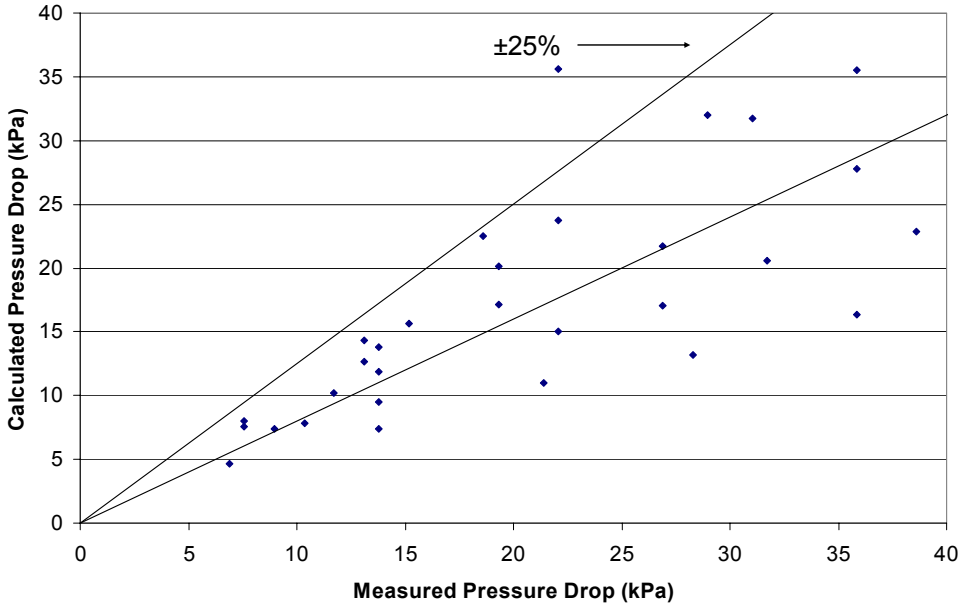

Figure 7-2. Predicted refrigerant pressure drop vs. experimentally measured pressure drop of microchannel heat exchangers used for validation

7.2 Validation of Wire-and-Tube Condenser Model

An initial validation of the wire-and-tube condenser model for forced convection heat transfer on the air side was performed using experimentally determined data. The data was measured for 3 different condensers—one condenser with airflow perpendicular to the tubes and parallel to the wires and two condensers with airflow perpendicular to both the tubes and the wires. Two test cases were measured for each condenser.

The experimental results were compared to simulations using both of the forced convection air-side heat transfer coefficients—namely the correlations developed by Hoke *et al*. (1997) and by Lee *et al*. (2001). The correlation developed by Lee *et al*. provided more accurate results. The correlation developed by Hoke *et al*. was found to underpredict the heat transfer coefficient. This result is in agreement with the findings by Lee *et al*. Therefore, the air-side heat transfer coefficient from Lee *et al*. was used for the validation study.

On the refrigerant side, the Gnielinski (1976) correlation was used to calculate the single-phase heat transfer coefficient. The correlation developed by Cavallini and Zecchin (1974), given in the Appendix, was used to calculate the heat transfer coefficient during condensation. For the calculation of the friction factor the correlation developed by Churchill (Chisholm, 1983) was used for single-phase refrigerant and the Lockhart-Martinelli (1949) correlation was used for two-phase refrigerant.

The normalized results of the validation are presented in Figure 7-3 and Figure 7-4. The results have been normalized in order to prevent the disclosure of

any condenser specifications. As shown in Figure 7-3, the heat load was predicted very accurately, with all of the heat load data points being predicted within 2.0%, with an average error of 1.0%. The normalized refrigerant pressure drop results are shown in Figure 7-4. All of the pressure drop data points were predicted within 20% with an average error of 3.8% and an average absolute error of 7.0%.

The accuracy of the model, as exemplified by these two figures, is very promising. However, as mentioned previously, only six data points were used in the validation. In the future, more validation studies of the wire-and-tube condenser model should be performed with more data points over a wider range of geometries and flow parameters.

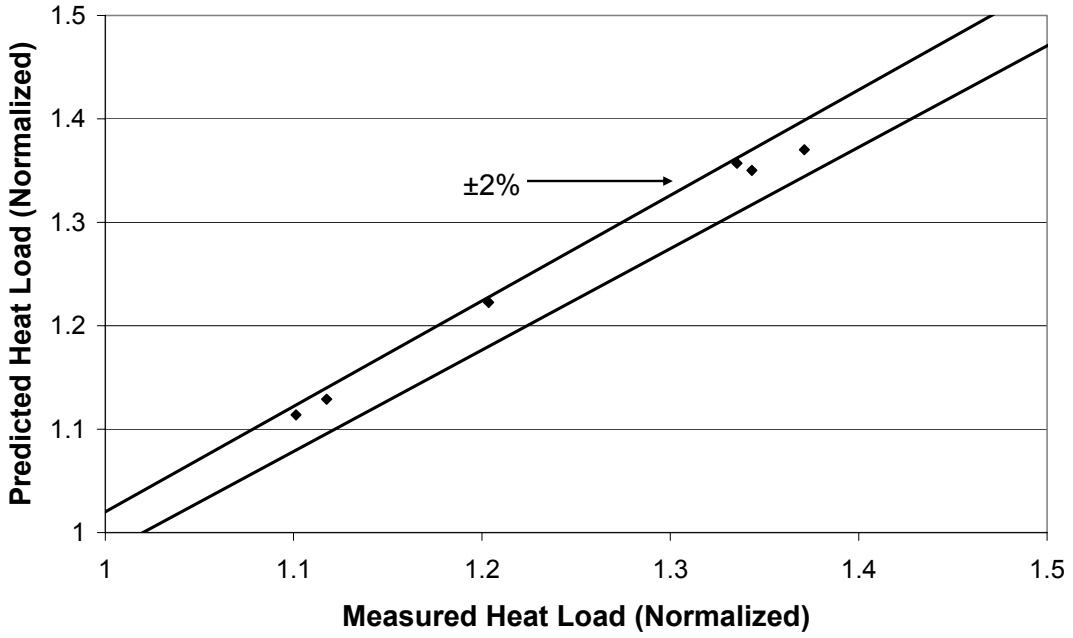

Figure 7-3. Predicted heat load vs. experimentally measured heat load of wire-and-tube condensers used for validation

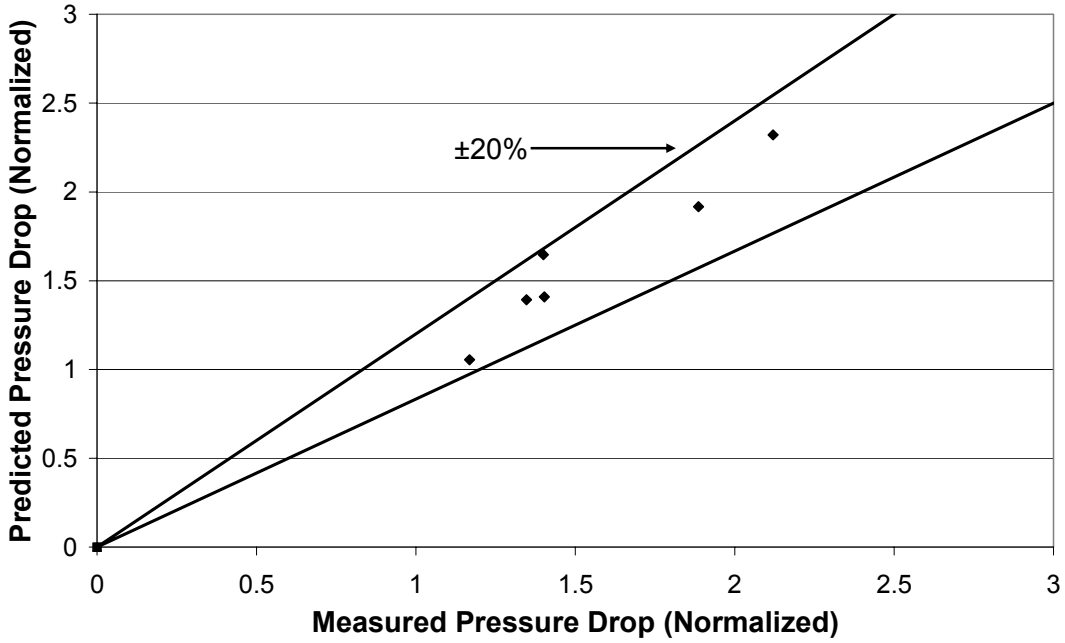

Figure 7-4. Predicted pressure drop vs. experimentally measured pressure drop of wire-and-tube condensers used for validation

7.3 Validation of Refrigerant-Oil Mixture Model

The refrigerant-oil mixture model described in Chapter 6 was used to model the heat load and oil retention of evaporators and condensers. In order to validate the model, the predicted results were then compared with experimental results obtained by Cremaschi (2004).

As a part of his experimental work, Cremaschi measured oil retention in round tube plate fin evaporators and condensers by injecting oil into the refrigerant flow at the inlet of a heat exchanger and then collecting the oil in an oil accumulator at the outlet of the heat exchanger. The oil retention in a heat exchanger could then be calculated as the difference between the oil injection flow rate and the rate of increasing oil volume in the oil accumulator. The experiments focused on three

different oils: mineral oil (MO) as well as the synthetic lubricants polyolester (POE) and polyalkylene glycole (PAG). Oil retention tests were performed with R-22/MO, R-410A/MO, R-410A/ POE, R-134a/POE, and R-134a/PAG mixtures. The oil mass fraction was varied between 1 and 8% by weight of the total mass flow rate of the refrigerant-oil mixture. The refrigerant mass flow rates were also varied between 42 and 60 g/s.

The results from modeling the oil retention in the evaporator are shown in Figure 7-5. As discussed before, the void fraction model by Premoli *et al*. (1971) provided the most accurate predictions for the oil retention. The average absolute error of all of the oil retention predictions was about 21%, and 72% of the data points were predicted within ±29%.

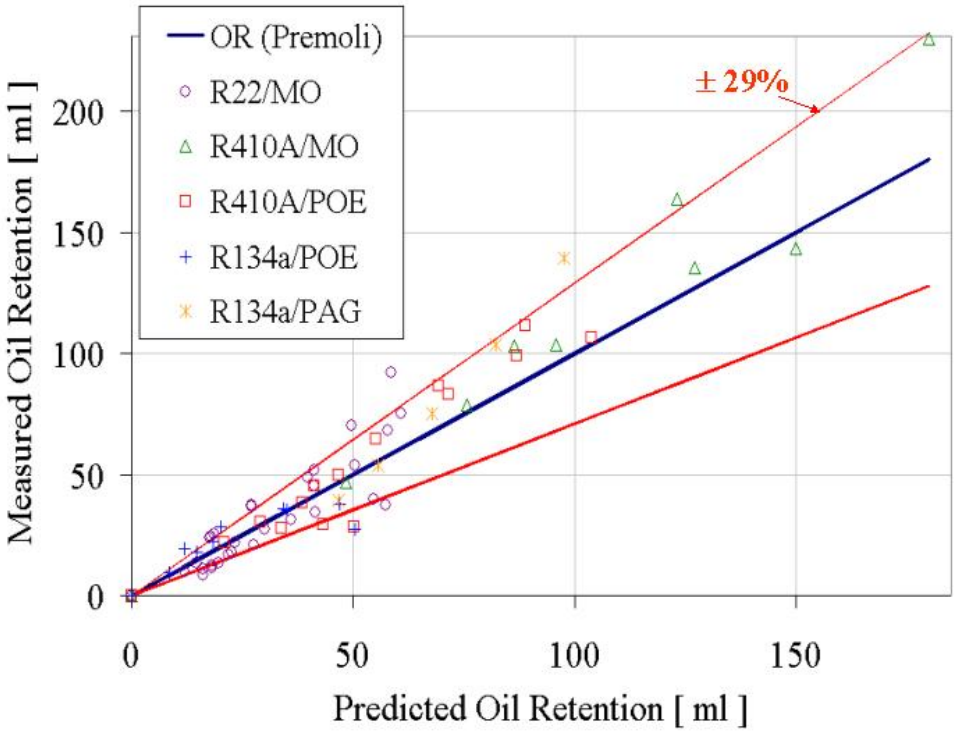

Figure 7-5. Experimentally measured oil retention vs. predicted oil retention in the evaporator (from Cremaschi, 2004)

CoilDesigner provides segment-by-segment output data, so detailed results for the oil retention, mixture quality, and local oil mass fraction can be obtained. Figure 7-6 shows these three quantities with respect to the dimensionless length of the evaporator. The local oil retention is plotted in dimensionless form, which is calculated as the ratio of the local oil retention volume over the maximum oil retention in a segment in the evaporator. The results shown in this figure are for the evaporator modeled with R-134a/PAG and an oil mass fraction of 2.4%. The tube circuitry of the evaporator is shown at the top of the figure. Of considerable note are the two kinks in the mixture quality curve corresponding to the points where the refrigerant-oil mixture flows from one column of tubes to the next. CoilDesigner predicts a change in the rate of increase of the mixture quality at these two points. This is to be expected because, as the fluid approaches the warmer inlet air, the refrigerant should evaporate at a greater rate. As can also be seen in Figure 7-6, the local oil mass fraction in the liquid mixture starts with a low value at the inlet to the evaporator because most of the refrigerant is in the liquid phase. As the refrigerant evaporates along the length of the heat exchanger, the oil remains in the liquid phase, so the local oil mass fraction increases. Closer to the outlet of the evaporator, most of the refrigerant has evaporated, so the local oil mass fraction is much higher. As a result, the viscosity of the liquid refrigerant-oil mixture is much higher towards the outlet of the heat exchanger, so most of the oil was retained in the last section of the evaporator.

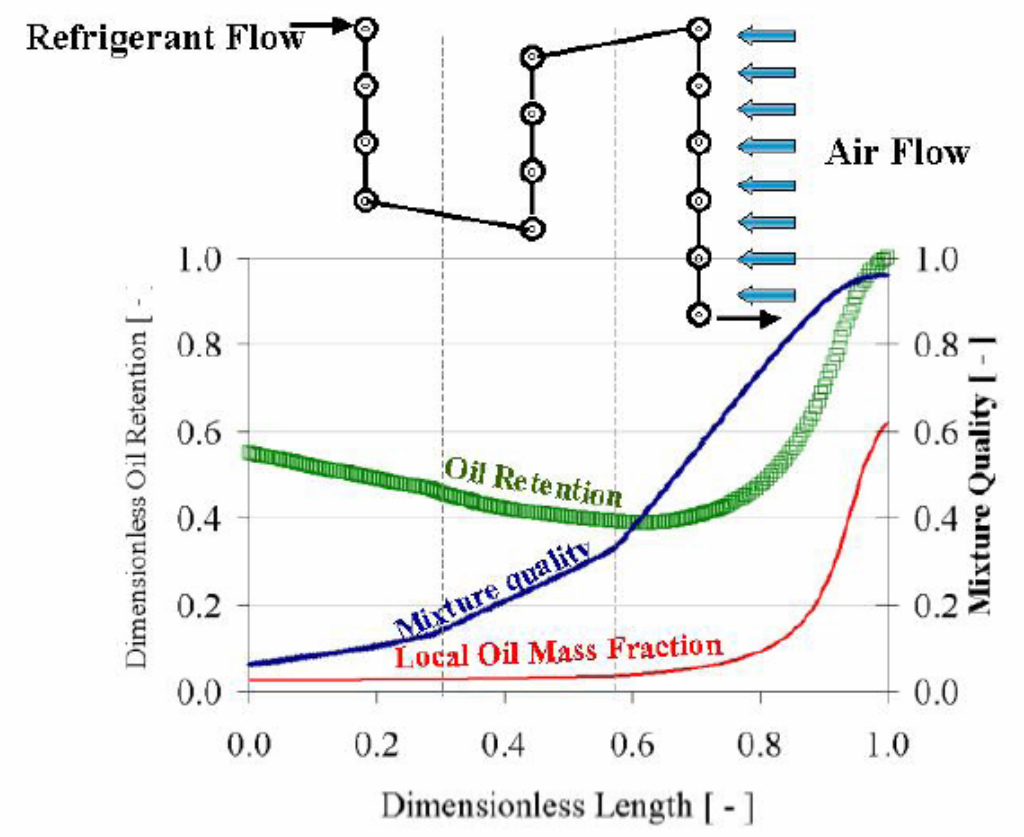

Figure 7-6. Calculated oil retention, mixture quality, and local oil mass fraction in an evaporator with R-134a/PAG at OMF=2.4% (from Cremaschi, 2004)

In addition to the oil retention, the heat load results of the evaporator were also compared with the experimental results. The heat load was predicted accurately with all of the data points predicted with an average absolute error of 12%.

The modeling results for the condenser are presented in Figure 7-7. The average absolute error for all of the oil retention data points was 23%, and about 70% of the data points were predicted within ±30%.

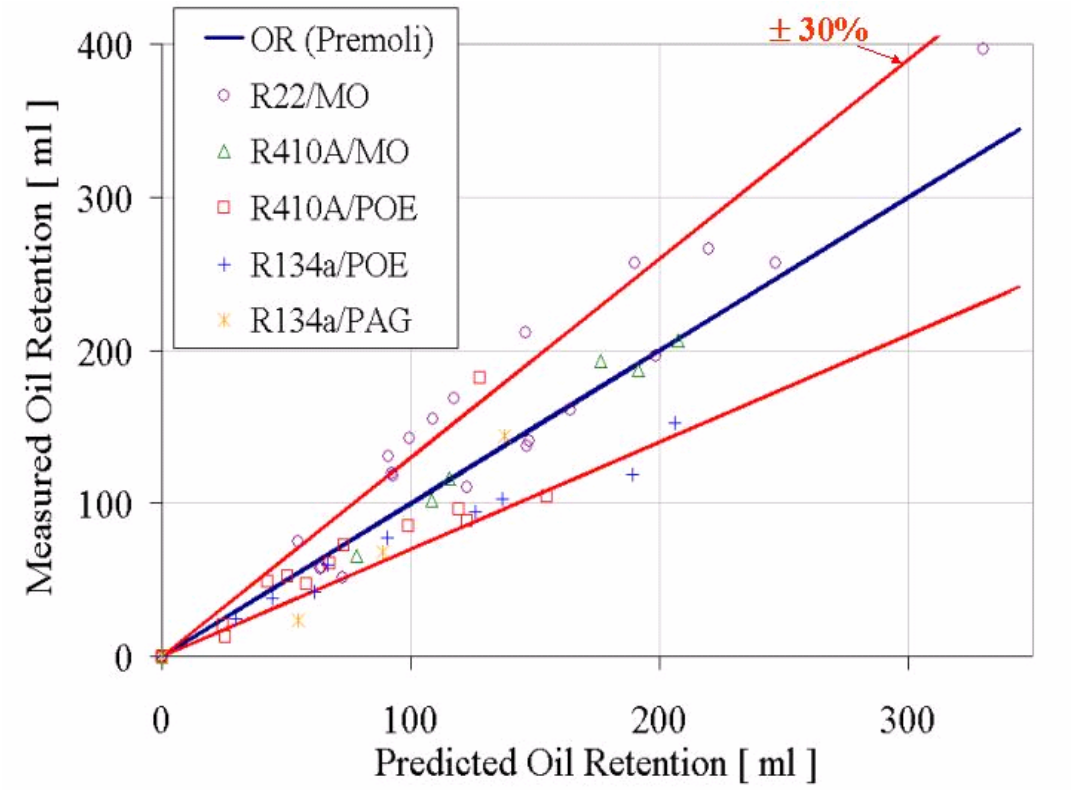

Figure 7-7. Experimentally measured oil retention vs. predicted oil retention for the condenser (from Cremaschi, 2004)

7.4 Optimization Study of Wire-and-Tube Condenser

One of the major motivations for creating heat exchanger models is to be able to perform optimization studies on heat exchangers in order to improve their capacity, efficiency, cost, and volume. The wire-and-tube condenser model was used to perform an optimization study to improve the cost and heat load of a wire-and-tube condenser that is currently used by a refrigerator manufacturer. Geometric parameters of the condenser were varied according to data provided by the manufacturer, but the number of different design possibilities was somewhat limited. Therefore, an optimization could be performed by searching the entire design space

for the best condenser designs. For this reason, more sophisticated techniques such as genetic algorithms were not necessary to perform the optimization study.

The following parameters were varied during the optimization study:

- Wire diameter
- Number of wires
- Tube diameter
- Horizontal and vertical distances between tubes

Each of these parameters was varied over a certain range of values, and every possible combination of parameters in those ranges was modeled. The cost for each test condenser was calculated according to cost information provided by the sponsor.

Two different optimization studies were performed. The first study used the same tube configuration as the existing condenser. The other optimization study involved modeling condensers with larger frontal face areas. This was accomplished by decreasing the number of columns of tubes in the direction of the airflow and increasing the number of rows of tubes in the vertical direction.

7.4.1 Optimization of Original Condenser

As noted above, the first optimization was performed using the same tube configuration as the existing condenser. Therefore, the number of rows and the number of columns of were kept constant while the parameters listed above were varied. In all, a total of 448 possible condensers were modeled. The heat load and the cost of the test condensers were compared with those of the original condenser. Figure 7-8 shows the heat load results with respect to the cost for all of the possible

condensers. The heat load and the cost have been normalized to prevent the disclosure of any proprietary data, so the original condenser has a value of 1 for both values.

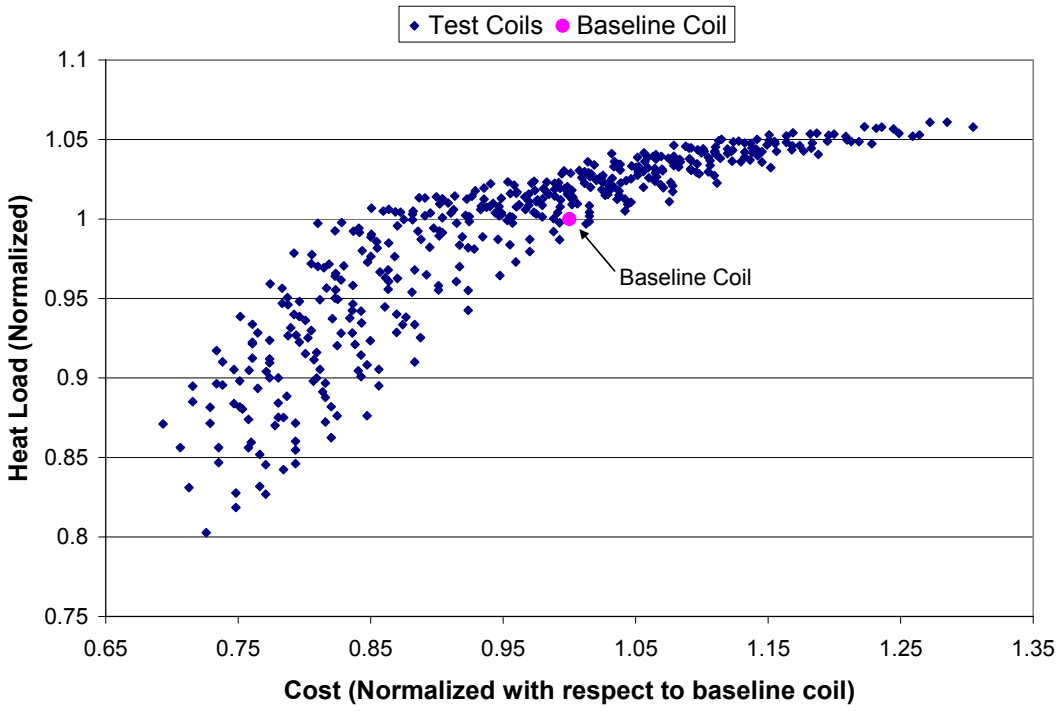

Figure 7-8. Heat load vs. cost of all test condensers in optimization of baseline condenser

In the optimization study, any condenser that was modeled as having a heat load greater than or equal to the baseline condenser and a cost less than or equal to the baseline condenser was considered to be better than the baseline condenser. Thus, in Figure 7-8, any point to left of and above the baseline condenser is considered to be an improvement. Of the 448 different condensers modeled, 147 of them fit these criteria. These better condensers are shown in Figure 7-9. Of particular note is the condenser at the far left of the graph. This condenser is modeled as having a heat load about 6.7% greater than the baseline condenser with a cost reduction of about 15%.

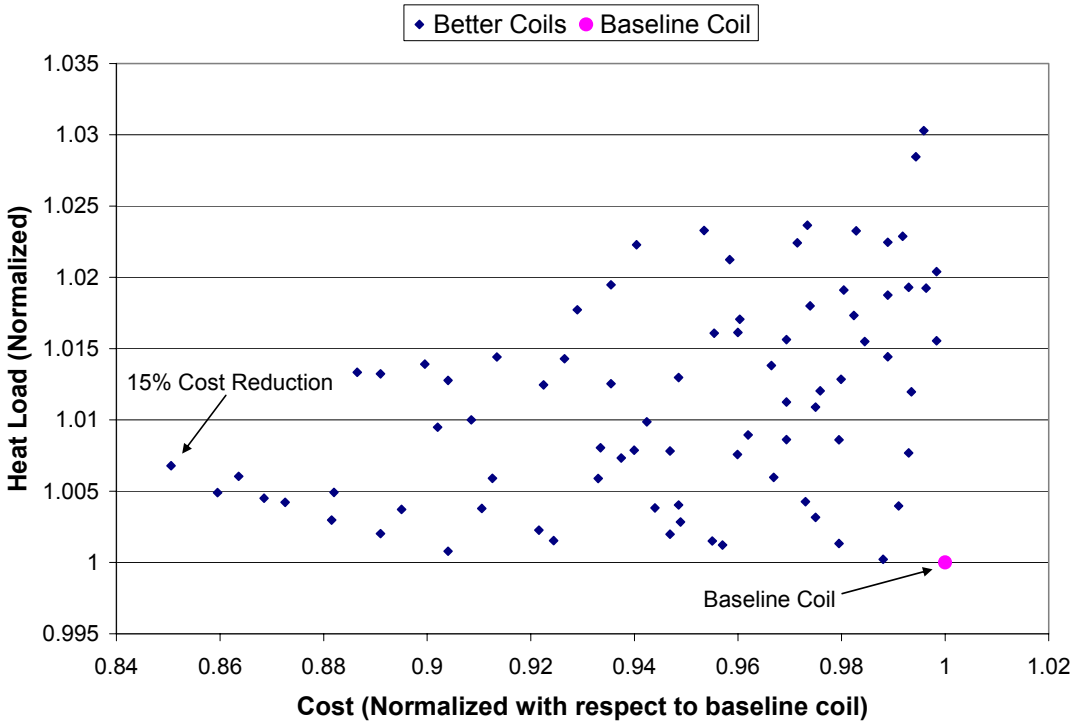

Figure 7-9. Heat load vs. cost for all better condensers in optimization of baseline condenser

7.4.2 Optimization of Condenser with Larger Face Area

Another optimization study was performed in which wire-and-tube condensers with larger frontal face areas were modeled, and the results were compared to the original condenser. The motivation behind modeling condensers with larger face areas was to design a condenser that could utilize more efficiently the space available to the condenser underneath the refrigerator. By filling more of the space available, better airflow through the condenser can be achieved, thereby increasing the heat transfer.

In order to model condensers with larger face areas, the number of columns in the direction of the airflow was reduced and the number of rows in the vertical direction was increased. It was assumed that for a larger face area, a larger fan would

be necessary. However, larger fans require more power to rotate at the same speed as a smaller fan. Therefore, in order to maintain or improve the efficiency of the entire refrigeration system, the speed of the new fan should be decreased to maintain the same power consumption as the original fan. The fan speed and the air velocity for the larger fan were calculated using the following procedure with the ASHRAE Fan Laws (ASHRAE, 2000). First, the power of the new fan, W_1, was assumed to be equal to the power of the original fan, W_2. Fan Law 1c relates the power of one fan to the power of another fan:

$$W_1 = W_2\left(\frac{D_1}{D_2}\right)^5\left(\frac{N_1}{N_2}\right)^3\left(\frac{\rho_1}{\rho_2}\right) \tag{7.1}$$

Assuming constant fan power and constant air density, Eq. 7.1 reduces to the following equation for the speed of the new fan, N_1:

$$N_1 = N_2\left(\frac{D_2}{D_1}\right)^{5/3} \tag{7.2}$$

Once the fan speed of the new condenser is calculated, the volumetric flow rate of the new fan, Q_1, can be calculated according to Fan Law 1a:

$$Q_1 = Q_2\left(\frac{D_1}{D_2}\right)^3\left(\frac{N_1}{N_2}\right) \tag{7.3}$$

which reduces to the following equation when Eq. 7.2 is substituted into Eq. 7.3:

$$Q_1 = Q_2\left(\frac{D_1}{D_2}\right)^{4/3} \tag{7.4}$$

Once the volume flow rate of the air has been calculated, the average air velocity through the new condenser can be calculated according to the following equation:

$$v_{avg} = \frac{Q_1}{A_1} \tag{7.5}$$

This average air velocity is then set as the input to the new condenser under consideration.

In addition to varying the number of rows and columns of tubes and the fan diameter in this optimization study, the parameters mentioned previously were also varied. Thus, for each tube configuration, several different values were modeled for the wire diameter, the number of wires, the tube diameter, and the horizontal and vertical distances between tubes. A total of 1,344 different condensers were modeled, of which 219 were found to be better than the original condenser. The normalized heat load and cost results of all the condensers are shown in Figure 7-10.

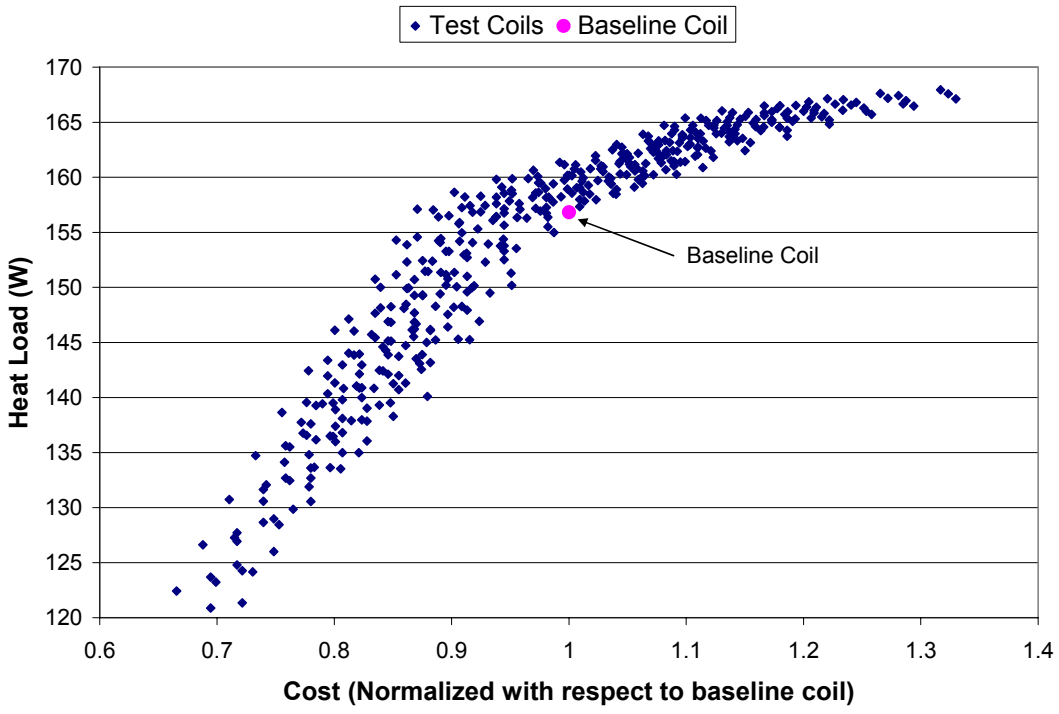

Figure 7-10. Heat load vs. cost of all test condensers in optimization of condensers with larger face area

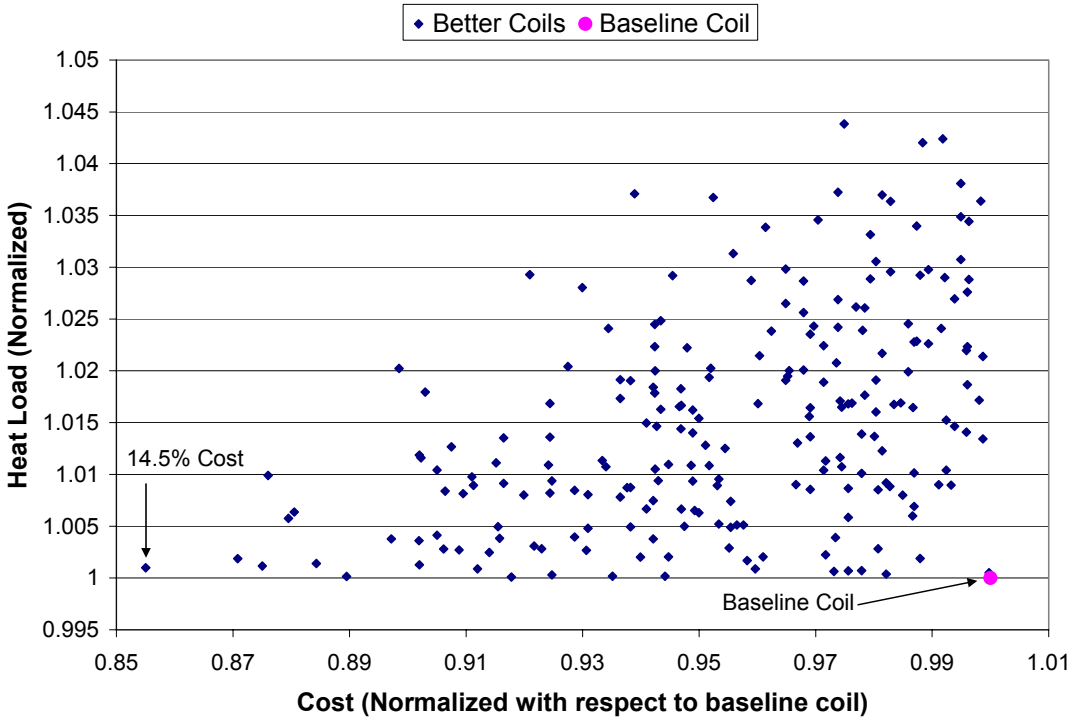

Figure 7-11. Heat load vs. cost for all better condensers in optimization of condensers with larger face area

Figure 7-11 shows the condensers that were modeled to be better than the original condenser. Of particular note in this optimization study is the point at the far left of Figure 7-11. This condenser was modeled to have a heat load slightly greater than the original condenser with a cost 14.5% less than the original condenser.

The company for which this optimization work was performed has since built a few condenser prototypes based on the results of the optimization. The company has reportedly obtained good results with a couple of the condenser designs. Though no details have been provided as far as which condensers provided better results, this news from the company is encouraging and provides motivation to perform other heat exchanger optimization studies with CoilDesigner.

Chapter 8 Conclusions

Several advances have been made to CoilDesigner to increase its modeling capabilities. The main motivation behind the work detailed in this thesis has been to improve the simulation and optimization capabilities of the heat exchanger design tool. The major advances and conclusions of this thesis are summarized in the Table 8-1 and then in the sections that follow.

Table 8-1. Summary of modeling capabilities added to CoilDesigner and work performed in relation to this thesis

	Models Included/Work Performed	**Comments**
Heat Exchanger Models	○ Wire-and-tube condenser model – Forced convection model – Natural convection model ○ Flat tube heat exchanger model	The models existing prior to the current research were: ○ Round tube plate fin ○ Microchannel
Void Fraction Models	○ Homogeneous model ○ Slip-ratio-correlated models ○ Lockhart-Martinelli parameter correlated models ○ Mass-flux-dependent models	Void fraction models were not previously available in CoilDesigner. Multiple correlations of each type of void fraction model have been included.
Refrigerant-Oil Mixture Model	○ Property calculations of refrigerant-oil mixtures ○ Heat load model accounting for temperature glide ○ Heat transfer coefficient and pressure drop correlations accounting for refrigerant-oil mixture properties	
Validation and Optimization Studies	○ Validation of microchannel heat exchanger model ○ Validation of wire-and-tube condenser model ○ Validation of refrigerant-oil mixture model ○ Optimization of wire-and-tube	Previously, the round tube plate fin model was the only model that had been validated.

	condenser	
Additional Modeling Capabilities	○ Louvered fins for RTPF, microchannel, and flat tube heat exchangers ○ Slit fins for RTPF heat exchangers ○ Serpentine microchannel heat exchanger model ○ Bend pressure drop for RTPF and serpentine microchannel and flat tube heat exchangers ○ Header pressure drop for microchannel heat exchangers with parallel flow ○ Carbon dioxide heat transfer coefficient and pressure drop correlations	For the most part, these modeling capabilities have not been described in detail in this thesis. Extensive literature searches have been performed to find correlations appropriate for these additional modeling capabilities.

8.1 New Heat Exchanger Models

Prior to the work presented in this thesis, CoilDesigner was capable of modeling two types of heat exchanger, namely round tube plate fin (RTPF) and microchannel heat exchangers. As a part of the research detailed in this thesis, models for wire-and-tube condensers and flat tube heat exchangers have been developed, thereby doubling the total number of heat exchanger models.

8.1.1 Wire-and-Tube Condenser Model

Wire-and-tube condensers are often used in domestic refrigerators. This type of heat exchanger employs either natural convection or forced convection heat transfer on the air side. A literature search has been performed to find correlations to calculate the air-side heat transfer coefficient, and models for both types of convection have been incorporated into CoilDesigner.

Natural Convection Wire-and-Tube Condenser Model

The natural convection model for wire-and-tube condensers includes the heat transfer due to natural convection as well as the heat transfer due to radiation. Correlations by Tanda and Tagliafico (1997) have been implemented to calculate convective and radiative heat transfer coefficients on the air side. An iterative method suggested by Bansal and Chin (2003) has been implemented to calculate the heat load.

Forced Convection Wire-and-Tube Condenser Model

The forced convection model includes the capability of modeling two different airflow configurations—airflow perpendicular to the tubes and to the wires as well as airflow perpendicular to the tubes and parallel to the wires. Correlations developed by Hoke *et al*. (1997) and by Lee *et al*. (2001) have been included to calculate the air-side heat transfer coefficient. Just as in the round tube plate fin heat exchanger model, the ε-NTU method is used to calculate the heat load in the forced convection model.

8.1.2 Flat Tube Heat Exchanger Model

The ability to model flat tube heat exchangers has also been incorporated into CoilDesigner. Flat tube heat exchangers are often used for automotive applications such as radiators and charge air coolers. The new solver allows for the following different geometric and fluid flow characteristics: serpentine and parallel fluid flow,

plate fins and corrugated fins, and inline and staggered tube configurations. Again, the ε-NTU is used to calculate the heat load. However, new air-side correlations for heat transfer and pressure drop were researched and implemented.

8.2 Additional Fluid Modeling Capabilities

8.2.1 Void Fraction Models and Charge Calculation

Accurate void fraction models are necessary to provide accurate charge calculations for a heat exchanger. Therefore, a comprehensive literature search has been performed for void fraction models. The models can be grouped into four different categories—homogeneous models, slip-ratio-correlated models, Lockhart-Martinelli parameter correlated models, and mass-flux-dependent models. A rather large number of void fraction models has been included in CoilDesigner because it is difficult to obtain experimental charge data with which to compare predicted results.

8.2.2 Modeling of Oil Effects and Oil Retention

Oil is an integral part of vapor compression systems and it can have a significant impact on the heat transfer and pressure drop in heat exchangers. The ability to model the effects of oil has been included in CoilDesigner. In order to model refrigerant-oil mixtures accurately, methods have been included to calculate the properties of refrigerant-oil mixtures as a function of the oil mass concentration. Refrigerant-oil mixtures behave like zeotropic mixtures because there is a temperature glide during the evaporation and condensation processes. Thus, the heat transfer with the air results in a latent heat load component and a sensible heat load

component in the refrigerant-oil mixture. A model introduced by Thome (1995) that accounts for the temperature glide is used to model the change in enthalpy of the refrigerant-oil mixture. Heat transfer coefficient and pressure drop correlations have also been included that account for the presence of oil.

8.3 Validation and Optimization Studies

Validation studies of the microchannel heat exchanger model and the wire-and-tube condenser model have been performed. A study has also been performed to determine the predictive capabilities of the model accounting for the effects of oil on heat exchanger performance. Finally, CoilDesigner has been used to perform optimization studies to design a more efficient and cost-effective wire-and-tube condenser. The results from these validation and optimization studies are summarized below.

8.3.1 Validation of Microchannel Heat Exchanger Model

A validation study of the microchannel heat exchanger has been performed. Experimental results from 35 tests on 8 different heat exchangers were compared with predicted results. The predictions were quite encouraging as 80% of the heat load data points were predicted within 2.25%, and the average absolute error for all of the heat load data points was 1.6%. For the refrigerant pressure drop, 54.3% of the data points were predicted within 25%, and the average absolute error for all data points was 25.9%.

8.3.2 Validation of Wire-and-Tube Condenser Model

A validation of the forced convection wire-and-tube condenser model has also been performed. Experimental data was collected from 3 different condensers—one condenser with airflow perpendicular to the tubes and parallel to the wires and two condensers with airflow perpendicular to both the tubes and the wires. During the validation study, a comparison was made between the air-side heat transfer coefficient correlations developed by Hoke *et al*. (1997) and Lee *et al*. (2001). The Lee *et al*. correlation was found to predict the heat transfer coefficient more accurately, so it was used for the validation study. The heat load data points of the wire-and-tube condensers were predicted within 2.0%, and the average error was only 1.0%. All of the pressure drop data points were predicted within 20% with an average absolute error of 7.0%.

8.3.3 Validation of Oil Retention Model

Experimental data obtained by Cremaschi (2004) was used to perform a validation of the oil retention model that was implemented in CoilDesigner. Oil retention was modeled in an evaporator and a condenser for R-22/MO, R-410A/MO, R-410A/ POE, R-134a/POE, and R-134a/PAG mixtures. For the evaporator, the average absolute error of all of the oil retention predictions was about 21%, and 72% of the data points were predicted within ±29%. Meanwhile, for the condenser, the average absolute error for all of the oil retention data points was 23%, and about 70% of the data points were predicted within ±30%.

8.3.4 Optimization of Wire-and-Tube Condenser

Two optimization studies were performed for a wire-and-tube condenser that is currently in use in domestic refrigerators. In the optimization studies, condensers were modeled using the entire design space specified by the manufacturer in order to find the best possible condensers given certain geometric constraints. In the first optimization study, condensers with the same tube circuitry as the original heat exchanger were modeled, but the wire diameter, the number of wires, the tube diameter, and the distances between the tubes were varied. Of the condensers modeled, 147 were found to provide a heat load greater than or equal to the original condenser with a cost less than or equal to the original condenser. One condenser in particular was modeled to provide a heat load about 6.7% greater than the original condenser with a cost reduction of about 15%

In the second optimization study, condensers with larger frontal face areas were modeled in order to enhance the airflow through the condensers. The number of tube columns in the direction of the airflow was reduced and the number of tube rows in the vertical direction was increased. Of the condensers modeled in this study, 219 were found to provide a higher heat load at a lesser cost compared to the original condenser. One condenser in particular was modeled to have a heat load slightly greater than the original condenser with a cost 14.5% less than the original condenser.

Chapter 9 Future Work

- Implement two-phase pressure drop and heat transfer coefficient correlations based on flow pattern maps
- Research and implement refrigerant-side heat transfer coefficient and pressure drop correlations developed specifically for flat tubes
- Obtain experimental data and perform validation studies for the natural convection wire-and-tube condenser model and for the flat tube model
- Obtain experimental charge data and compare the prediction capabilities of the multiple void fraction models that have been included in CoilDesigner

Appendix

A.1 Air-Side Heat Transfer Coefficient Correlations for Flat Tubes

The air-side heat transfer coefficient correlations that follow are in the form of the Colburn factor, j. Once the Colburn factor has been calculated, the air-side heat transfer coefficient can be calculated according to the following equation:

$$h = \frac{j \cdot G \cdot c_{p,air}}{Pr_{air}^{2/3}} \tag{A.1}$$

Kays and London (1984)

Heun and Dunn (1996) used data from Kays and London (1984) to develop a correlation to calculate the Colburn factor for flat tube heat exchangers with corrugated fins:

$$j = 0.0538 \cdot Re_{Dh}^{-0.401} \tag{A.2}$$

where Re_{Dh} is the Reynolds number based on the hydraulic diameter on the air side:

$$Re_{Dh} = \frac{G \cdot D_h}{\mu_{air}} \tag{A.3}$$

The air-side hydraulic diameter is calculated according to the following equation:

$$D_h = \frac{4 A_{min} L_{flow}}{A_{total}} \tag{A.4}$$

where A_{min} is the minimum free flow area for the air, L_{flow} is the heat exchanger depth in the airflow direction, and A_{total} is the total surface area of the tubes and fins.

Chang and Wang (1997)

Chang and Wang (1997) developed an empirical correlation to calculate the Colburn factor for corrugated louvered fins for flat tube heat exchangers:

$$j = Re_{Lp}^{-0.49} \cdot \left(\frac{L_\theta}{90}\right)^{0.27} \left(\frac{F_p}{L_p}\right)^{-0.14} \left(\frac{F_l}{L_p}\right)^{-0.29} \left(\frac{T_{w,out}}{L_p}\right)^{-0.23} \left(\frac{L_l}{L_p}\right)^{0.68} \left(\frac{S_t}{L_p}\right)^{-0.28} \left(\frac{F_t}{L_p}\right)^{-0.05} \quad \text{(A.5)}$$

A.2 Air-Side Pressure Drop Correlations for Flat Tubes

The air-side pressure drop correlations that follow are in the form of the Fanning friction factor, *f*. Once the friction factor has been calculated, the air-side pressure drop can be calculated according to the following equation:

$$\Delta P = f \cdot \frac{A_{total}}{A_{min}} \cdot \frac{G^2}{2\rho_{air}} \quad \text{(A.6)}$$

Kays and London (1984)

Heun and Dunn (1996) also used data from Kays and London (1984) to develop a correlation to calculate the friction factor for flat tube heat exchangers with corrugated fins:

$$f = 1.298 \cdot Re_{Dh}^{-0.429} \quad \text{(A.7)}$$

where Re_{Dh} is the Reynolds number based on the hydraulic diameter of the air side, given by Eq. A.3.

Chang *et al.* (2000)

$$f = f_1 \cdot f_2 \cdot f_3 \quad \text{(A.8)}$$

where, if the Reynolds number based on the louver pitch is less than 150, the quantities f_1, f_2, and f_3 are calculated according to the following equations:

$$f_1 = 14.39 \cdot Re_{Lp}^{-0.805 \cdot F_p / F_l} \cdot \left[\ln\left(1 + \frac{F_p}{L_p} \right) \right]^{3.04} \tag{A.9}$$

$$f_2 = \left[\ln\left(\left(\frac{F_t}{F_p} \right)^{0.48} + 0.9 \right) \right]^{-1.435} \cdot \left(\frac{D_h}{L_p} \right)^{-3.01} \cdot \left[\ln\left(0.5 \cdot Re_{Lp} \right) \right]^{-3.01} \tag{A.10}$$

$$f_3 = \left(\frac{F_p}{L_l} \right)^{-0.308} \cdot \left(\frac{F_d}{L_l} \right)^{-0.308} \cdot \exp\left(-0.1167 \cdot \frac{S_t}{T_{h,out}} \right) \cdot L_\theta^{0.35} \tag{A.11}$$

On the other hand, if the Reynolds number is between 150 and 5,000, then f_1, f_2, and f_3 are calculated according to the following equations:

$$f_1 = 4.97 \cdot Re_{Lp}^{0.6049 - 1.064 / L_\theta^{0.2}} \cdot \left[\ln\left(\left(\frac{F_t}{F_p} \right)^{0.5} + 0.9 \right) \right]^{-0.527} \tag{A.12}$$

$$f_2 = \left[\frac{D_h}{L_p} \cdot \ln\left(0.3 \cdot Re_{Lp} \right) \right]^{-2.966} \cdot \left(\frac{F_p}{L_l} \right)^{-0.7931 \cdot \frac{S_t}{H}} \tag{A.13}$$

$$f_3 = \left(\frac{S_t}{T_{h,out}} \right)^{-0.0446} \cdot \left[\ln\left(1.2 + \left(\frac{L_p}{F_p} \right)^{1.4} \right) \right]^{-3.553} \cdot L_\theta^{-0.477} \tag{A.14}$$

A.3 Refrigerant-Side Heat Transfer Coefficient Correlations

Cavallini and Zecchin (1974)

$$h = 0.05 \cdot \mathrm{Re}_{eq}^{0.8} \cdot \left(\frac{\mu_{liq} \cdot c_{p,liq}}{k_{liq}} \right)^{0.33} \cdot \frac{k_{liq}}{D} \tag{A.15}$$

where

$$Re_{eq} = Re_{liq} + Re_{vap} \cdot \frac{\mu_{vap}}{\mu_{liq}} \cdot \left(\frac{\rho_{liq}}{\rho_{vap}} \right)^{0.5} \tag{A.16}$$

where the liquid and vapor Reynolds numbers are defined as follows:

$$Re_{liq} = \frac{4 \cdot \dot{m} \cdot (1 - x)}{\pi \cdot D \cdot \mu_{liq}} \tag{A.17}$$

$$Re_{vap} = \frac{4 \cdot \dot{m} \cdot x}{\pi \cdot D \cdot \mu_{vap}} \tag{A.18}$$

A.4 Void Fraction Models

The void fraction models implemented in CoilDesigner are included in this section. If more than one reference is included for a model, then the original reference could not be found, and so the model was taken from another reference.

A.4.1 Void Fraction Models for Round Tubes

Homogenous Void Fraction Model

As discussed in Chapter 5, the homogeneous void fraction is calculated according to the following equation:

$$\alpha = \frac{1}{1 + \left(\frac{1 - x}{x} \right) \frac{\rho_{vap}}{\rho_{liq}}} \tag{A.19}$$

Slip-Ratio-Correlated Void Fraction Models

As also discussed in Chapter 5, the slip-ratio-correlated models use the following equation to calculate the void fraction:

$$\alpha = \frac{1}{1 + \left(\frac{1-x}{x}\right)\frac{\rho_{vap}}{\rho_{liq}} \cdot S} \tag{A.20}$$

All of the slip-ratio-correlated void fraction models were developed for annular flow.

Thom (1964)

Thom (1964) developed slip ratios for steam-water flow at different pressures based on experimental data. Ahrens (1983) generalized the slip ratios to use with other fluids through the use of the following property index:

$$P.I. = \left(\frac{\mu_{liq}}{\mu_{vap}}\right)^{0.2} \cdot \frac{\rho_{vap}}{\rho_{liq}} \tag{A.21}$$

Table A-1. Slip ratios *S* based on property index *P.I.* generalized from Thom's steam-water data (1964) by Ahrens (1983)

P.I.	0.00116	0.0154	0.0375	0.0878	0.187	0.446	1.0
S	6.45	2.48	1.92	1.57	1.35	1.15	1.00

In order to use the Thom slip ratio in CoilDesigner, a curve-fit equation was developed based on the data in Table A-1. The curve-fit equation was generated using the software tool TableCurve 2D® (SYSTAT, 2002) and has the following form:

$$S = c_1 + c_2 \cdot P.I. + c_3 \cdot P.I.^3 + \frac{c_4}{\sqrt{P.I.}} + \frac{c_5}{P.I.^2} \tag{A.22}$$

where the coefficients c_1 through c_2 are shown in Table A-2.

Table A-2. Coefficients for use with Eq. A.22, the curve-fit equation developed to calculate the slip ratio for the Thom void fraction model

c_1	0.938959893346381
c_2	-0.178509024795173
c_3	0.0479370689134024
c_4	0.191578314482982
c_5	-1.52972456792532E-07

Zivi (1964)

Zivi (1964) developed an analytical model for the slip ratio based on the assumption of minimum entropy production under the ideal conditions of zero wall friction and zero entrainment. The slip ratio is given by the following equation:

$$S = \left(\frac{\rho_{vap}}{\rho_{liq}} \right)^{-1/3} \tag{A.23}$$

Based on experimental data, Zivi found that the actual void fraction is bracketed between the predictions using this slip ratio and using the homogeneous void fraction model.

Smith (1969; Tandon *et al*., 1985)

$$S = K + (1-K) \cdot \left[\frac{\frac{\rho_{liq}}{\rho_{vap}} + K\left(\frac{1-x}{x} \right)}{1 + K\left(\frac{1-x}{x} \right)} \right]^{1/2} \tag{A.24}$$

Smith found good agreement with experimental data by setting $K = 0.4$.

Rigot (1973; Rice, 1987)

Rigot (1973) made the assumption of a constant slip ratio:

$$S = 2 \tag{A.25}$$

Lockhart-Martinelli Parameter Correlated Void Fraction Models

In the following void fraction models, semi-empirical correlations have been developed to describe the void fraction as a function of the Lockhart-Martinelli parameter:

$$X_{tt} = \left(\frac{1-x}{x}\right)^{0.9} \sqrt{\left(\frac{\mu_{liq}}{\mu_{vap}}\right)^{0.2} \cdot \frac{\rho_{vap}}{\rho_{liq}}} \tag{A.26}$$

Lockhart-Martinelli (1949; Rice, 1987)

Lockhart and Martinelli (1949) did not actually develop a void fraction correlation, but they presented void fraction data as a function of X_{tt}. Based on their data, Wallis (1969) and, later, Domanski and Didion (1983) developed the following equations to calculate the void fraction (Rice, 1987):

$$\alpha = \left(1 + X_{tt}^{0.8}\right)^{-0.378} \qquad \text{for } X_{tt} \le 10 \tag{A.27}$$

$$\alpha = 0.823 - 0.157 \ln X_{tt} \quad \text{for } X_{tt} > 10 \tag{A.28}$$

Baroczy (1966; Rice, 1987; Koyama *et al*., 2004)

Baroczy (1966) presented void fraction data as a function of both X_{tt} and the property index given in Eq. A.21. The liquid void fraction data (i.e., 1-α) Baroczy measured is presented in the Table A-3:

Table A-3. Liquid void fraction (1-α) data presented by Baroczy (1966)

		X_{tt}										
		0.01	0.04	0.1	0.2	0.5	1	3	5	10	30	100
PI	0.00002				0.0012	0.009	0.068	0.17	0.22	0.30	0.47	0.71
	0.0001			0.0015	0.0054	0.030	0.104	0.23	0.29	0.38	0.57	0.79
	0.0004		0.0022	0.0072	0.1800	0.066	0.142	0.28	0.35	0.45	0.67	0.85
	0.001	0.0018	0.0066	0.0170	0.0345	0.091	0.170	0.32	0.40	0.50	0.72	0.88
	0.004	0.0043	0.0165	0.0370	0.0650	0.134	0.222	0.39	0.48	0.58	0.80	0.92
	0.01	0.0050	0.0210	0.0475	0.0840	0.165	0.262	0.44	0.53	0.63	0.84	0.94
	0.04	0.0056	0.0250	0.0590	0.1050	0.215	0.330	0.53	0.63	0.72	0.90	0.96
	0.1	0.0058	0.0268	0.0640	0.1170	0.242	0.380	0.60	0.70	0.78	0.92	0.98
	1	0.0060	0.0280	0.0720	0.1400	0.320	0.500	0.75	0.85	0.90	0.94	0.994

Based on the data presented by Baroczy, the following correlation has since been developed to calculate the void fraction (Koyama *et al*., 2004):

$$\alpha = \left[1 + \left(\frac{1-x}{x} \right)^{0.74} \left(\frac{\rho_{vap}}{\rho_{liq}} \right)^{0.65} \left(\frac{\mu_{liq}}{\mu_{vap}} \right)^{0.13} \right]^{-1} \tag{A.29}$$

Mass-Flux-Dependent Void Fraction Models

Hughmark (1962)

The Hughmark void fraction model (1962) was developed for the bubble flow regime in vertical upward flow. However, Hughmark found the correlation to work well for other flow regimes in horizontal tubes. The void fraction is calculated according to the following equation:

$$\alpha = \frac{K_H}{1 + \left(\frac{1-x}{x} \right) \frac{\rho_{vap}}{\rho_{liq}}} = K_H \beta \tag{A.30}$$

where β is simply the homogeneous void fraction given by Eq. A. and K_H is a function of the parameter Z, which is defined as

$$Z = \frac{Re_{\alpha}^{1/6} Fr^{1/8}}{y_l^{1/4}} \tag{A.31}$$

where Re_{α} is a void-fraction-weighted Reynolds number,

$$Re_{\alpha} = \frac{D \cdot G}{\mu_{liq} + \alpha \cdot (\mu_{vap} - \mu_{liq})} \tag{A.32}$$

Fr is the Froude number,

$$Fr = \frac{v^2}{gD} = \frac{1}{gD}\left(\frac{Gx}{\beta \rho_{vap}}\right)^2 \tag{A.33}$$

where g is the acceleration due to gravity and y_{liq} is the liquid volume fraction:

$$y_{liq} = \frac{1}{1 + \left(\frac{x}{1-x}\right)\frac{\rho_{liq}}{\rho_{vap}}} = 1 - \beta \tag{A.34}$$

Hughmark provided data for K_H as a function of Z, reproduced here in Table A-4.

Table A-4. Hughmark flow parameter K_H as a function of Z (1962)

Z	K_H
1.3	0.185
1.5	0.225
2	0.325
3	0.490
4	0.605
5	0.675
6	0.720
8	0.767
10	0.780
15	0.808
20	0.830
40	0.880
70	0.930
130	0.980

For the purposes of calculating K_H in CoilDesigner, Hughmark's data was used to develop a curve-fit equation. The curve-fit equation was developed using TableCurve 2D® (SYSTAT, 2002) and has the following form:

$$K_H = \frac{c_1 + c_2 \cdot Z + c_3 \cdot Z^2 + c_4 \cdot Z^3 + c_5 \cdot Z^4}{1 + c_6 \cdot Z + c_7 \cdot Z^2 + c_8 \cdot Z^3 + c_9 \cdot Z^4} \tag{A.35}$$

Table A-5. Coefficients for use with Eq. A.35, the curve-fit equation developed to calculate the Hughmark flow parameter K_H as a function of Z

c_1	-0.102620597649546
c_2	0.221766018541533
c_3	0.00426608255825076
c_4	0.00716611986632982
c_5	9.0414594961056E-05
c_6	0.0532071133347019
c_7	0.0267848812904344
c_8	0.00852408911446845
c_9	8.1662804078423E-05

Because the Reynolds number is a function of the void fraction, α, and the void fraction is, in turn, a function of the Reynolds number, the void fraction equation is an implicit function. Therefore, the set of equations defined by Eq. A.30 through Eq. A.35 must be solved iteratively. Ridders' method (Press *et al*., 1992) with brackets 0 and 1 was chosen to perform the numerical iteration and solve for the void fraction. Since the Hughmark void fraction model must be solved using an iterative process, this model requires a larger amount of computation time than the other void fraction models and can, therefore, slow down the modeling of a heat exchanger.

Rouhani and Axelsson (1970)

Rouhani and Axelsson (1970) developed their void fraction model to be valid throughout the different boiling regions, without discontinuities during the transitions between different boiling regions.

$$\alpha = \frac{x}{\rho_{vap}}\left\{C\left[\frac{x}{\rho_{vap}}+\frac{1-x}{\rho_{liq}}\right]+\frac{1.18}{G}\cdot\left[\frac{\sigma\cdot g\left(\rho_{liq}-\rho_{vap}\right)}{\rho_{liq}^2}\right]^{1/4}\right\}^{-1} \tag{A.36}$$

where $C = 1.12$ for G > 200 kg/(m^2 s), $C = 1.54$ for G < 200 kg/(m^2 s), σ is the surface tension of the liquid, and g is the acceleration due to gravity.

Premoli *et al*. (1971; Kakaç, 1991)

The void fraction model developed by Premoli *et al*. (1971) is also known as the CISE correlation. The Premoli void fraction model is a slip-ratio-correlated model for annular flow, so the void fraction is calculated by substituting the slip ratio into Eq. A.20. However, as opposed to the other slip ratio models, the Premoli slip ratio is dependent on the mass flux and is calculated according to the following equations:

$$S = 1 + E_1 \cdot \left(\frac{y}{1+yE_2} - yE_2\right)^{0.5} \tag{A.37}$$

$$E_1 = 1.578 \cdot Re_{liq}^{-0.19}\left(\frac{\rho_{liq}}{\rho_{vap}}\right)^{0.22} \tag{A.38}$$

$$E_2 = 0.0273 \cdot We_{liq} \cdot Re_{liq}^{-0.51}\left(\frac{\rho_{liq}}{\rho_{vap}}\right)^{-0.08} \tag{A.39}$$

$$y = \frac{\beta}{1-\beta} \tag{A.40}$$

where, again, β is the homogeneous void fraction, given in Eq. A.. In this case, the liquid Reynolds and Weber numbers are calculated according to the following equations:

$$Re_{liq} = \frac{GD}{\mu_{liq}} \tag{A.41}$$

$$We_{liq} = \frac{G^2 D}{\sigma \rho_{liq}} \tag{A.42}$$

where σ is the surface tension of the liquid.

Tandon, Varma, and Gupta (1985)

The Tandon *et al*. void fraction model (1985) is an analytical model for two-phase annular flow. The model accounts for the effect of wall friction through the use of the Lockhart-Martinelli parameter. The liquid Reynolds number is used and is calculated according to Eq. A.41 above. The void fraction is calculated according to the following equation for $50 < Re_{liq} < 1125$:

$$\alpha = 1 - 1.928 \cdot Re_{liq}^{-0.315} \cdot \left[F\left(X_{tt}\right)\right]^{-1} + 0.9293 \cdot Re_{liq}^{-0.63} \cdot \left[F\left(X_{tt}\right)\right]^{-2} \tag{A.43}$$

and according to the following equation for $Re_{liq} > 1125$:

$$\alpha = 1 - 0.38 \cdot \mathrm{Re}_{liq}^{-0.088} \cdot \left[F\left(X_{tt}\right)\right]^{-1} + 0.0361 \cdot \mathrm{Re}_{liq}^{-0.176} \cdot \left[F\left(X_{tt}\right)\right]^{-2} \tag{A.44}$$

where $F(X_{tt})$ is defined by the following equation:

$$F\left(X_{tt}\right) = 0.15\left(X_{tt}^{-1} + 2.85 X_{tt}^{-0.476}\right) \tag{A.45}$$

Yashar *et al*. (2001)

The Yashar *et al*. (2001) void fraction model was developed for stratified and annular flow. It accounts for gravitational dominated effects through the use of the Froude rate parameter and for the viscous drag effects through the use the Lockhart-Martinelli parameter:

$$\alpha = \left(1 + \frac{1}{Ft} + X_{tt}\right)^{-0.321} \tag{A.46}$$

where Ft is the Froude rate

$$Ft = \left[\frac{G^2 x^3}{(1-x)\rho_{vap}^2 gD}\right]^{0.5} \tag{A.47}$$

Harms, *et al*. (2003)

The void fraction model developed by Harms *et al*. (2003) for annular flow is an empirical model that accounts for the effect of momentum eddy diffusivity damping at the interface between the liquid and vapor. The authors obtained good agreement with experimental results at moderate mass fluxes.

$$\alpha = \left[1 - 10.06 \cdot Re_{liq}^{-0.875}\left(1.74 + 0.104 \cdot Re_{liq}^{0.5}\right)^2 \cdot \left(1.376 + \frac{7.242}{X_{tt}^{1.655}}\right)^{-1/2}\right]^2 \tag{A.48}$$

where X_{tt} is again calculated according to Eq. A.26, and Re_{liq}, in this case, is calculated according to the following equation:

$$Re_{liq} = \frac{(1-x)GD}{\mu_{liq}} \tag{A.49}$$

A.4.2 Void Fraction Models for Microchannel Tubes

Armand (1946)

Although the Armand void fraction model (1946) was developed for round tubes, it was found to work well for microchannel tubes with a hydraulic diameter of about 1 mm by Chung and Kawaji (2004). The correlation simply multiplies a constant times the homogeneous void fraction.

$$\alpha = \frac{0.833}{1+\left(\frac{1-x}{x}\right)\frac{\rho_{vap}}{\rho_{liq}}} \tag{A.50}$$

Ali, Sadatomi, and Kawaji (1993)

Ali *et al*. (1993) also found the void fraction in narrow channels to be predicted well by multiplying a constant times the homogeneous void fraction:

$$\alpha = \frac{0.8}{1+\left(\frac{1-x}{x}\right)\frac{\rho_{vap}}{\rho_{liq}}} \tag{A.51}$$

Their model was developed using data from experimental investigations with channels of width 0.778 mm and 1.465 mm between two flat plates.

References

Achaichia, A., and Cowell, T.A., 1988, Heat Transfer and Pressure Drop Characteristics of Flat Tube and Louvered Plate Fin Surfaces, *Experimental Thermal and Fluid Science*, Vol. 1, No., 2, pp. 147-157.

Ali, M.I., Sadatomi, M., and Kawaji, M., 1993, Adiabatic Two-Phase Flow in Narrow Channels Between Two Flat Plates, *The Canadian Journal of Chemical Engineering*, Vol. 71, pp. 657-666.

Ahrens, F.W., 1983, Heat pump modeling, simulation and design, *Heat Pump Fundamentals: Proceedings of the NATO Advanced Study Institute on Heat Pump Fundamentals, Espinho, Spain (i.e. Portugal), 1980*, ed. J. Berghmans, Martinus Nijhoff Publishers, The Hague, Netherlands.

Armand, A.A., 1946, The resistance during the movement of a two-phase system in horizontal pipes, *Izv. Vses. Teplotekh*, Inst. 1, pp. 16-23, AERA-Lib/Trans 828.

ASHRAE, 2000, *ASHRAE Handbook—HVAC Systems and Equipment*, Atlanta, GA, pp. 18.4-18.5.

Bansal, P.K., and Chin, T.C., 2003, Modelling and optimisation of wire-and-tube condenser, *International Journal of Refrigeration*, Vol. 26, pp. 601-613.

Baroczy, C.J., 1966, A systematic correlation for two-phase pressure drop, *Chemical Engineering Progress Symposium Series*, Vol. 62, No. 62, pp. 232-249.

Cavallini, A., and Zecchin, R., A dimensionless correlation for heat transfer in forced convection condensation, *Proceedings of the Sixth International Heat Transfer Conference*, Vol. 3, pp. 309-313.

Chaddock, J.B., and Mathur, A.P., 1980, Heat transfer to oil-refrigerant mixtures evaporating in tubes, *Proceedings of the Second Multi-Phase Flow and Heat Transfer Symposium-Workshop*, Vol. 2, pp. 861-884, Miami Beach, FL.

Chang, Y.J., Hsu, K.C., Lin, Y.T., and Wang, C.C., 2000, A generalized friction correlation for louver fin geometry, *International Journal of Heat and Mass Transfer*, Vol. 43, No. 12, pp. 2237-2243.

Chang, Y.J., and Wang, C.C., 1996, Air side performance of brazed aluminum heat exchangers, *Journal of Enhanced Heat Transfer*, Vol. 3, No. 1, pp. 15-28.

Chang, Y.J., and Wang, C.C., 1997, A generalized heat transfer correlation for louver fin geometry, *International Journal of Heat and Mass Transfer*, Vol. 40, No. 3, pp. 533-544.

Chisholm, D., 1983, *Two-Phase Flow in Pipelines and Heat Exchangers*, Longman Inc., New York.

Chung, P.M.Y., and Kawaji, M., 2004, The effect of channel diameter on adiabatic two-phase flow characteristics in microchannels, *International Journal of Multiphase Flow*, Vol. 30, pp. 735-761.

Cremaschi, L., 2004, Experimental and Theoretical Investigation of Oil Retention in Vapor Compression Systems, Ph.D. Dissertation, Department of Mechanical Engineering, University of Maryland, College Park, MD.

Cremaschi, L., Schwentker, R.A., and Radermacher, R., In Press, Modeling of Oil Retention in the Suction Line and Evaporator of Air Conditioning Systems, *HVAC&R Research Journal*.

Davenport, D.J., 1983, Correlation for heat transfer and flow friction characteristics of louvered fin, *AIChE Symposium Series*, Vol. 79, No. 225, pp. 19-27.

Dillen, E.L., and Webb, R.L., 1994, Rationally Based Heat Transfer and Friction Correlations for the Louver Fin Geometry, *1994 SAE International Congress & Exposition*, Detroit, MI, Paper 940504.

Dittus, F.W., and Boelter, L.M.K., 1930, Heat Transfer in Automobile Radiators of the Tubular Type, *University of California Publications on Engineering*, Vol. 2, p. 443, Berkeley, CA. Reprinted in *International Communications in Heat and Mass Transfer*, 1985, Vol. 12, No. 1, pp. 3-22.

Dobson, M.K., and Chato, J.C., 1998, Condensation in Smooth Horizontal Tubes, *Transactions of the ASME, Journal of Heat Transfer*, Vol. 120, pp. 193-213.

Fang, X., Bullard, C.W., and Hrnjak, P.S., 2001, Modeling and Analysis of Gas Coolers, *ASHRAE Transactions*, Vol. 107, No. 1, Report 4411.

Filippov, L.P., and Novoselova, N.S., 1955, Thermal conductivity of normal liquid solutions, *Vestnik Moskov. Gos. Univ., Ser. Fiz.*, Vol. 3, pp. 37-40.

Gnielinski, V., 1976, New equations for heat and mass transfer in turbulent pipe and channel flow, *International Chemical Engineering*, Vol. 16, No. 2, pp. 359-368.

Harms, T.M., Li, D., Groll, E.A., and Braun, J.E., 2003, A void fraction model for annular flow in horizontal tubes, *International Journal of Heat and Mass Transfer*, Vol. 46, pp. 4051-4057.

Heun, M.K., and Dunn, W.E., 1996, Principles of Refrigerant Circuiting with Application to Microchannel Condensers: Part 2—The Pressure Drop Effect and the Cross-Flow Heat Exchanger, *ASHRAE Transactions*, Vol. 102, No. 2, pp. 382-393.

Hilpert, R., 1933, Wärmeabgabe von geheizten Drähten und Rohren im Luftstrom, *Forsch. Gebiete Ingenieurw*, Vol. 4, pp. 215-224.

Hoke, J.L., Clausing, A.M., and Swofford, T.D., 1997, An Experimental Investigation of Convective Heat Transfer From Wire-On-Tube Heat Exchangers, *Transactions of the ASME, Journal of Heat Transfer*, Vol. 119, pp. 348-356.

Hughmark, G.A., 1962, Holdup in gas-liquid flow, *Chemical Engineering Progress*, Vol. 58, No. 4, pp. 62-65.

Jensen, M.K., and Jackman, D.L., 1984, Predictions of Nucleate Pool Boiling Heat Transfer Coefficients of Refrigerant-Oil Mixtures, *Transactions of the ASME, Journal of Heat Transfer*, Vol. 106, pp. 184-190.

Jiang, H., Aute, V., and Radermacher, R., 2002, A User-Friendly Simulation and Optimization Tool for Design of Coils, *Proceedings of the 9th International Refrigeration and Air Conditioning Conference at Purdue*, Purdue University, West Lafayette, IN, Paper R5-1.

Jiang, H., 2003, Development of a Simulation and Optimization Tool for Heat Exchanger Design, Ph.D. Dissertation, Department of Mechanical Engineering, University of Maryland, College Park, MD.

Jung, D.S., and Radermacher, R., 1989, Prediction of pressure drop during horizontal annular flow boiling of pure and mixed refrigerants, *International Journal of Heat and Mass Transfer*, Vol. 32, No. 12, pp. 2435-2446.

Kakaç, S., 1991, *Boilers, Evaporators, and Condensers*, John Wiley & Sons, Inc., New York.

Kakaç, S., and Liu, H., 2002, *Heat Exchangers: Selection Rating and Thermal Design*, 2nd edition, CRC Press, Boca Raton, FL.

Kays, W.M., and Crawford, M.E., 1993, *Convective Heat and Mass Transfer*, 3rd edition, McGraw-Hill, Inc., New York.

Kays, W. M., and London, A. L., 1984, *Compact Heat Exchangers*, 3rd edition, McGraw-Hill, New York.

Kim, M. H., and Bullard, C. W., 2001, Development of a microchannel evaporator model for a CO2 air-conditioning system, Energy, Vol. 26, No. 10, pp. 931-948.

Kim, N.H., Youn, B., and Webb, R.L., 1999, Air-Side Heat Transfer and Friction Correlations for Plain Fin-and-Tube Heat Exchangers With Staggered Tube

Arrangements, *Transactions of the ASME, Journal of Heat Transfer*, Vol. 121, pp. 662-667.

Koyama, S., Lee, J., and Yonemoto, R., 2004, An investigation on void fraction of vapor-liquid two-phase flow for smooth and microfin tubes with R134a at adiabatic condition, *International Journal of Multiphase Flow*, Vol. 30, pp. 291-310.

Lee, T.H., Yun, J.Y., Lee, J.S., Park, J.J., and Lee, K.W., 2001, Determination of airside heat transfer coefficient on wire-on-tube type heat exchanger, *International Journal of Heat and Mass Transfer*, Vol. 44, pp. 1767-1776.

Lemmon, E.W., McLinden, M.O., and Huber, M.L., 2002, *REFPROP – Reference Fluid Thermodynamic and Transport Properties*, National Institute of Standards and Technology, Boulder, CO.

Lockhart, R.W., Martinelli, R.C., 1949, Proposed correlation of data for isothermal two-phase two-component flow in pipes, *Chemical Engineering Progress*, Vol. 45, No. 1, pp. 39-48.

McQuiston, F., and Parker, J., 1994, *Heating, Ventilating, and Air Conditioning: Analysis and Design*, 4th edition, John Wiley & Sons, Inc, New York.

Myers, G.E., 1998, *Analytical Methods in Conduction Heat Transfer*, 2nd edition, AMCHT Publications, Madison, WI.

Ortiz, T.M., and Groll, E.A., 2002, Validation of a New Model for Predicting the Performance of Carbon Dioxide as a Refrigerant for Residential Air Conditioners, *Proceedings of the 9th International Refrigeration and Air Conditioning Conference at Purdue*, Purdue University, West Lafayette, IN, Paper R11-2.

Ortiz, T.M., Li, D., and Groll, E.A., 2003, Evaluation of the Performance Potential of CO2 as a Refrigerant in Air-to-Air Conditioners and Heat Pumps: System Modeling and Analysis, *Air-Conditioning and Refrigeration Technology Institute Report*, ARTI-21CR/610-10030.

Pettersen, J., 2004, Flow vaporization of CO_2 in microchannel tubes, *Experimental Thermal and Fluid Science*, Vol. 28, pp. 111-121.

Pettersen, J., Rieberer, R., and Leister, A., 2000, Heat Transfer and Pressure Drop Characteristics of Super-Critical Carbon Dioxide in Microchannel Tubes Under Cooling, *Proceedings of the 4th IIR Gustav Lorentzen Conference on Natural Working Fluids*, IIF-IIR Commission B1, B2, E1, and E2, Purdue University, West Lafayette, IN.

Pettersen, J., Rieberer, R., and Munkejord, S.T., 2000a, Heat Transfer and Pressure Drop Characteristics of Evaporating Carbon Dioxide in Microchannel Tubes,

Proceedings of the 4th IIR Gustav Lorentzen Conference on Natural Working Fluids, IIF-IIR Commission B1, B2, E1, and E2, Purdue University, West Lafayette, IN.

Pettersen, J., Rieberer, R., and Munkejord, S.T., 2000b, Heat Transfer and Pressure Drop for Flow of Supercritical and Subcritical CO_2 in Microchannel Tubes, Final Technical Report, United States Army, Contract Number N-68171-99-M-5674, Issued by SINTEF Energy Research and Norwegian University of Science and Technology.

Premoli, A., Francesco, D., and Prina, A., 1971, A dimensionless correlation for determining the density of two-phase mixtures, *La Termotecnica*, Vol. 25, pp. 17-26.

Press, W.H., Teukolsky, S.A., Vetterling, W.T., and Flannery, B.P., 1992, *Numerical Recipes in C: The Art of Scientific Computing*, 2nd edition, Cambridge University Press, New York, online at http://www.library.cornell.edu/nr/cbookcpdf.html.

Quadir, G.A., Krishnan, G.M., and Seetharamu, K.N., 2002, Modeling of wire-on-tube heat exchangers using finite element method, *Finite Elements in Analysis and Design*, Vol. 38, pp. 417-434.

Rice, C.K., 1987, The Effect of Void Fraction Correlation and Heat Flux Assumption on Refrigerant Charge Inventory Predictions, *ASHRAE Transactions*, Vol. 93, No. 1, Report 3035.

Rigot, G., 1973, Fluid capacity of an evaporator in direct expansion, *Chaud-Froid-Plomberie*, No. 328, pp. 133-144 (English translation, ORNL-tr-5217, Oak Ridge National Laboratory, Oak Ridge, TN).

Rouhani, S.Z., and Axelsson, E., 1970, Calculation of Void Volume Fraction in the Subcooled and Quality Boiling Regions, *International Journal of Heat and Mass Transfer*, Vol. 13, pp. 383-393.

Rugh, J.P., Pearson, J.T., and Ramadhyani, S., 1992, A study of a very compact heat exchanger used for passenger compartment heating in automobiles, *Compact Heat Exchangers for Power and Process Industries*, ASME Symposium Series, ASME HTD Vol. 201, pp. 15-24.

Sahnoun, A., and Webb, R.L., 1992, Prediction of Heat Transfer and Friction for the Louver Fin Geometry, *Transactions of the ASME*, *Journal of Heat Transfer*, Vol. 114, pp. 893-900.

Schwentker, R.A., Aute, V.C., and Radermacher, R., 2005, Simulation and Design Tool for Wire-and-Tube Condensers, *IIR Conferences: Thermophysical Properties and Transfer Processes of Refrigerants*, Vicenza, Italy.

Schwentker, R.A., Aute, V.C., Radermacher, R., and Mercer, K.B., 2005, Simulation and Design Tool for Microchannel Heat Exchangers, *Fifth International Conference on Enhanced, Compact and Ultra-Compact Heat Exchangers: Science, Engineering and Technology*, Whistler, British Columbia, Canada.

Shah, M.M., 1979, A general correlation for heat transfer during film condensation inside pipes, *International Journal of Heat and Mass Transfer*, Vol. 22, No. 4, pp. 547-556.

Shah, R.K., and Sekuliç, D.P., 2003, *Fundamentals of Heat Exchanger Design*, John Wiley & Sons, Inc., Hoboken, NJ.

Shen, B., and Groll, E.A., 2003, Critical Literature Review of Lubricant Influence on Refrigerant Heat Transfer and Pressure Drop, *Air-Conditioning and Refrigeration Institute Report*, ARTI-21CR/611-20080.

Smith, S.L., 1969, Void fractions in two-phase flow: a correlation based upon an equal velocity head model, *Proceedings of the Institution of Mechanical Engineers*, Vol. 184, Pt. 1, No. 36, pp. 647-664.

Sunden, B., and Svantesson, J., Correlation of *j*- and *f*-factors for multilouvered heat transfer surfaces, *Proceedings of the Third UK National Conference on Heat Transfer*, pp. 805-811.

SYSTAT Software Inc., 2002, TableCurve 2D® Version 5.01, Port Richmond, CA.

Tagliafico, L., and Tanda, G., 1997, Radiation and natural convection heat transfer from wire-and-tube heat exchangers in refrigeration appliances, *International Journal of Refrigeration*, Vol. 20, No. 7, pp. 461-469.

Tanda, G., and Tagliafico, L., 1997, Free Convection Heat Transfer From Wire-and-Tube Heat Exchangers, *Transactions of the ASME, Journal of Heat Transfer*, Vol. 119, pp. 370-372.

Tandon, T.N., Varma, H.K., and Gupta, C.P., 1985, A void fraction model for annular two-phase flow, *International Journal of Heat and Mass Transfer*, Vol. 28, No. 1, pp. 191-198.

Thom, J.R.S., 1964, Prediction of Pressure Drop During Forced Circulation Boiling of Water, *International Journal of Heat and Mass Transfer*, Vol. 7, pp. 709-724.

Thome, J.R., 1995, Comprehensive Thermodynamic Approach to Modeling Refrigerant-Lubricating Oil Mixtures, *HVAC&R Research*, Vol. 1, No. 2, pp. 110-126.

Thome, J.R., 2003, On Recent Advances in Modeling of Two-Phase Flow and Heat Transfer, *Heat Transfer Engineering*, Vol. 24, No. 6, pp. 46-59.

Wang, C.C., Lee, W.S., and Sheu, W.J., 2001, A comparative study of compact enhanced fin-and-tube heat exchangers, *International Journal of Heat and Mass Transfer*, Vol. 44, pp. 3565-3573.

Yashar, D.A., Wilson, M.J., Kopke, H.R., Graham, D.M., Chato, J.C., and Newell, T.A., 2001, An Investigation of Refrigerant Void Fraction in Horizontal, Microfin Tubes, HVAC&R Research, Vol. 7, No. 1, pp. 67-82.

Yin, J.M., Bullard, C.W., and Hrnjak, P.S., 2001, R-744 gas cooler model development and validation, *International Journal of Refrigeration*, Vol. 24 No. 7, pp. 692-701.

Yokozeki, M.A., 1994, Solubility and viscosity of refrigerant-oil mixtures, *Proceedings of the 1994 International Refrigeration Conference at Purdue*, Purdue University, West Lafayette, IN, pp. 335-340.

Zivi, S.M., 1964, Estimation of Steady-State Steam Void-Fraction by Means of the Principle of Minimum Entropy Production, *Transactions of the ASME, Journal of Heat Transfer*, Vol. 86, pp. 247-252.

Žukauskas, A., 1972, Heat Transfer from Tubes in Crossflow, in *Advances in Heat Transfer*, Vol. 8, eds. J.P. Hartnett and T.F. Irvine, Jr., Academic Press, New York, pp.93-160.